The Plant Cell, Vol. 14, 2431–2450, October 2002, www.plantcell.org © 2002 American Society of Plant Biologists

A Cell-Specific, Prenylation-Independent Mechanism Regulates Targeting of Type II RACs

Meirav Lavy, Keren Bracha-Drori, Hasana Sternberg, and Shaul Yalovsky[1]

Department of Plant Sciences, Tel Aviv University, Ramat Aviv, Tel Aviv 69978, Israel

The RHO proteins, which regulate numerous signaling cascades, undergo prenylation, facilitating their interaction with membranes and with proteins called RHO·GDP dissociation inhibitors. It has been suggested that prenylation is required for RHO function. Eleven RHO-related proteins were identified in Arabidopsis. Eight of them are putatively prenylated. We show that targeting of the remaining three proteins, AtRAC7, AtRAC8, and AtRAC10, is prenylation independent, requires palmitoylation, and occurs by a cell-specific mechanism. AtRAC8 and AtRAC10 could not be prenylated by either farnesyltransferase or geranylgeranyltransferase I, whereas AtRAC7 could be prenylated by both enzymes in yeast. The association of AtRAC7 with the plasma membrane in plants did not require farnesyltransferase or a functional CaaX box. Recombinant AtRAC8 was palmitoylated in vitro, and inhibition of protein palmitoylation relieved the association of all three proteins with the plasma membrane. Interestingly, AtRAC8 and a constitutively active mutant, Atrac7mV^{15}, were not associated with the plasma membrane in root hair cells, whose elongation requires the localization of prenylated RHOs in the plasma membrane at the cell tip. Moreover, Atrac7mV^{15} did not induce root hair deformation, unlike its prenylated homologs. Thus, AtRAC7, AtRAC8, and AtRAC10 may represent a group of proteins that have evolved to fulfill unique functions.

INTRODUCTION

The RHO family of small GTP binding proteins consists of four distinctive subgroups known as Rho, Rac, CDC42, and a plant-specific subgroup called Rop or RAC (Van Aelst and D'Souza-Schorey, 1997; Hall, 1998; Winge et al., 2000; Zheng and Yang, 2000a). Rhos, Racs, and CD42 differentially regulate the actin cytoskeleton (reviewed by Hall, 1998). Rho GTPases also regulate several signaling cascades, including mitogen-activated protein kinase and phosphoinositide pathways (reviewed by Van Aelst and D'Souza-Schorey, 1997; Hall, 1998; Bar-Sagi and Hall, 2000; Bishop and Hall, 2000). In addition, members of the Rac family regulate the production of reactive oxygen species through the activation of NADPH oxidase (Bokoch, 1994).

RHOs undergo cycles of GTP-bound (on) and GDP-bound (off) states. A group of proteins known as GDP dissociation inhibitors (GDIs) form a complex with inactive GDP-bound Rho proteins and release them from the membrane to the cytosol. Upon activation, RHOs are released from the GDIs and bind to the membrane (Takahashi et al., 1997; Olofsson, 1999). Thus, GDIs play an essential role in the regulation of RHO activity.

RHOs undergo prenylation at a conserved C-terminal CaaX box motif (where C is Cys, a is usually an aliphatic residue, and X is one of several residues). After prenylation, the proteins undergo trimming of the aaX moiety and methylation on the free carboxylate of the isoprenyl Cys (Schafer and Rine, 1992; Zhang and Casey, 1996; Rodriguez-Concepcion et al., 1999a; Yalovsky et al., 1999). Some Rho proteins are palmitoylated further on Cys residues proximal to the CaaX box (Michaelson et al., 2001). Palmitoylation involves the attachment of palmitate or other saturated fatty acids to Cys residues by a reversible thioester bond (Linder, 2000).

In mammalian tissue culture cells, the subcellular localization of most RHO proteins is determined by their C-terminal hypervariable domains and by binding to RHO·GDI (Michaelson et al., 2001). The C-terminal hypervariable domain contains the CaaX box prenylation motif, a polybasic domain composed mainly of Lys residues, and, in some proteins, additional Cys residues that serve as acceptors for palmitoylation. Prenylation is required to direct proteins to the endoplasmic reticulum (Choy et al., 1999; Apolloni et al., 2000; Michaelson et al., 2001), whereas CaaX processing facilitates the targeting of proteins to their final destination in

[1] To whom correspondence should be addressed. E-mail shauly@tauex.tau.ac.il; fax 972-3-6406933.

Article, publication date, and citation information can be found at www.plantcell.org/cgi/doi/10.1105/tpc.005561.

the cell (Boyartchuk et al., 1997; Rodriguez-Concepcion et al., 2000; Bracha et al., 2002). The polybasic domain is required for plasma membrane targeting of K-RasB (Choy et al., 1999; Apolloni et al., 2000) and the efficient prenylation of proteins by geranylgeranyltransferase I (GGTase-I) (James et al., 1995; Caldelari et al., 2001). It probably plays a similar role in RHOs. Palmitoylation inhibits the interaction between RHOs and RHO·GDIs (Michaelson et al., 2001), directing proteins to the plasma membrane, and the partitioning of proteins into lipid rafts (Zacharias et al., 2002). Thus, the differential regulation of RHO targeting by various mechanisms appears to modulate specific cellular signaling cascades.

Plant RHOs have evolved as a distinct group known as Rops (Rhos from plants) by some researchers (Zheng and Yang, 2000a) and RACs by others (Winge et al., 2000). Rops/RACs regulate a wide array of cellular processes. These include the creation and maintenance of Ca^{2+} gradients needed to elongate the pollen tube and root hair cells (Li et al., 1999; Molendijk et al., 2001; Jones et al., 2002), the associated regulation of F-actin (Fu et al., 2001, 2002), and phosphoinositide signaling (Kost et al., 1999). Rops/RACs also regulate various hormone-mediated plant signaling and developmental processes (Li et al., 2001), the production of reactive oxygen species (Potikha et al., 1999; Park et al., 2000), and the associated pathogen-induced hypersensitive response (Schiene et al., 2000; Ono et al., 2001).

In Arabidopsis, 11 different Rop/RAC GTPases have been identified (Winge et al., 2000) (Figure 1). The last amino acids in the CaaX boxes of AtRAC7 and AtRAC8 are Ala and Asn, respectively, suggesting that they might be substrates of farnesyltransferase (FTase) rather than GGTase-I, like the remaining eight Rops/RACs. A third protein, called AtRAC10, is 95% identical to AtRAC8 but contains four additional amino acids downstream of an internal CaaX box. AtRAC7, AtRAC8, and AtRAC10 belong to a subfamily of the Rops/RACs that was formed by the addition of an exon at the 3′ end of the gene immediately downstream of the sequence encoding an internal CaaX box; this family is referred to as type II Rop/RAC (Winge et al., 2000). After transient expression, a maize homolog of AtRAC7 that does not have a functional CaaX box was localized to the plasma membrane, suggesting that prenylation is not involved in the targeting of this protein (Ivanchenko et al., 2000). Interestingly, a rice homolog belonging to this subfamily was found to elicit the pathogen-induced hypersensitive response (Ono et al., 2001).

Here, we present analyses of the subcellular localization and prenylation of AtRAC7, AtRAC8, and AtRAC10. The data show that AtRAC7, AtRAC8, and AtRAC10 differ in their ability to become prenylated. However, the plasma membrane localization of all three proteins is prenylation independent, requires palmitoylation, and depends on a plant cell–specific mechanism. Our results suggest that plants have evolved unique mechanisms for subcellular targeting and the regulation of type II RACS.

RESULTS

Structure and Subcellular Localization of AtRAC7, AtRAC8, and AtRAC10

The Arabidopsis Rop/RAC GTPases constitute a large protein family of 11 members. Sequence alignment shows the high percentage of conservation of these proteins (Figure 1A). Three members of the family, termed AtRAC7, AtRAC8, and AtRAC10, differ from the other eight members, mainly in the C-terminal hypervariable domain (Figure 1A). Detailed analysis of AtRAC7, AtRAC8, and AtRAC10 revealed two conserved Cys residues, an additional Cys in AtRAC7, and two conserved Gly residues (Figure 1B). AtRAC7 Cys-206 and AtRAC8 Cys-205 are part of potential CaaX boxes, whereas AtRAC10, which is 95% identical to AtRAC8, lacks a conserved prenylation motif because there are seven additional residues C terminal to Cys-208. AtRAC7 Cys-196, AtRAC8 Cys-199, and AtRAC10 Cys-202 align with the CaaX box Cys residues of all other known members of the Arabidopsis Rop/RAC proteins (Figure 1A), whereas the additional Cys residues, AtRAC7 Cys-203 and Cys-206, AtRAC8 Cys-205, and AtRAC10 Cys-208, are encoded by an additional exon located at the 3′ end of these three genes.

Because AtRAC7, AtRAC8, and AtRAC10 differ in their C terminus from all other members of the Rop/RAC family in Arabidopsis, their subcellular targeting and localization may be different. We raised several questions. What is the subcellular localization of AtRAC7, AtRAC8, and ATRAC10? Could AtRAC7 and AtRAC8 be prenylated, and if so, does prenylation affect their localization? Are AtRAC7, AtRAC8, and AtRAC10 also modified by palmitoylation? Finally, we wanted to determine what could be learned about the biological activity of these three proteins.

First, we defined the subcellular localization of AtRAC7, AtRAC8, and AtRAC10 using green fluorescent protein (GFP) fusion proteins. Fusions between GFP and RHO GTPases were shown to localize and function like their cognate native proteins (Michaelson et al., 2001; Molendijk et al., 2001). When expressed as an unmodified protein in leaf epidermal cells of *Nicotiana benthamiana*, GFP was distributed throughout the cytoplasm and the nucleus (Figure 2B). The same leaves were stained with 4′,6-diamidino-2-phenylindole to show the localization of nuclei (Figure 2A). GFPAtRAC8 was localized exclusively in the plasma membrane, as the GFP–differential interference contrast overlay image shows (Figure 2C). Similarly, GFPAtRAC7 also was localized only in the plasma membrane (Figure 2D). GFPAtRAC10 showed a different subcellular distribution. Most of the protein was localized in the plasma membrane, and a smaller fraction was observed in the nucleus (Figure 2D).

The subcellular localization of AtRAC7, AtRAC8, and AtRAC10 is atypical of RHO GTPases, which usually are

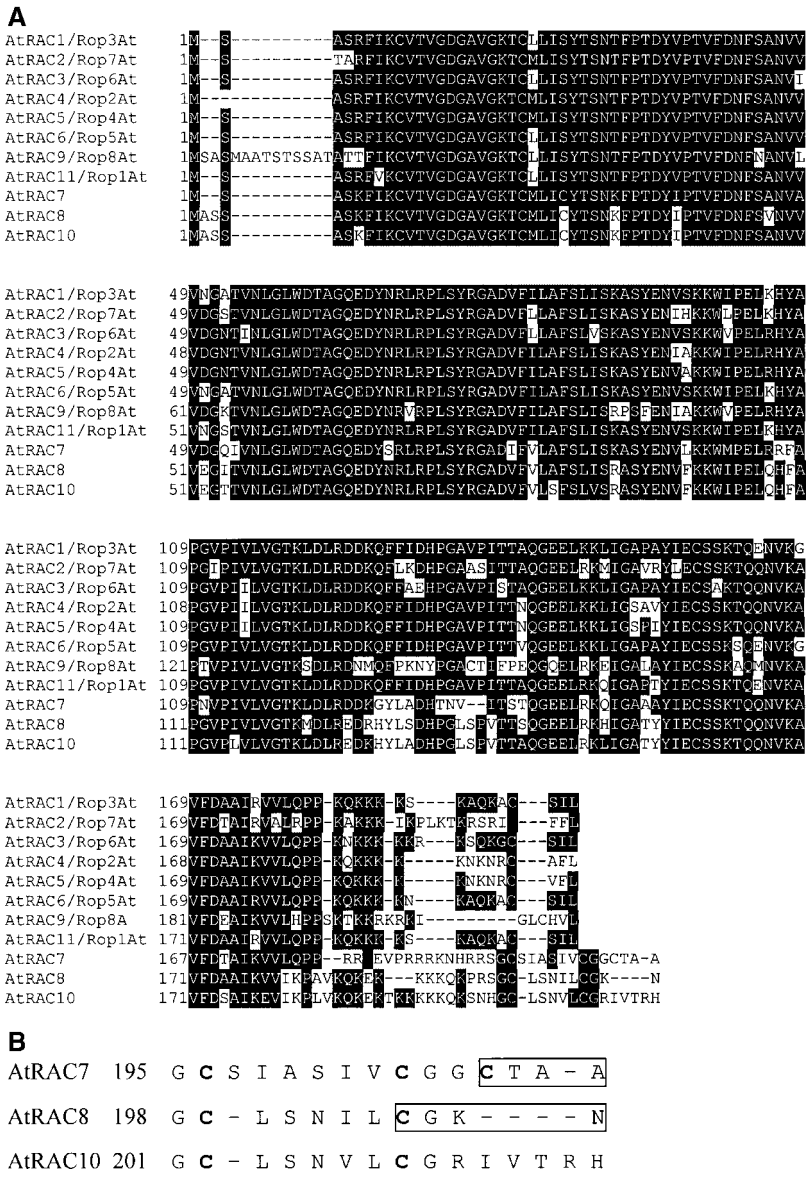

Figure 1. Sequence Alignment of Arabidopsis Rop/RAC GTPases.

(A) Alignment of 11 Arabidopsis Rops/RACs was made with the Clustal algorithm (LASERGENE software; DNASTAR, Inc., Madison, WI). Black boxes denote identical amino acids. Note the divergence of AtRAC7, AtRAC8, and AtRAC10 from the type I Rops/RACs at the C-terminal hypervariable domain.

(B) Alignment of the C-terminal hypervariable domains of AtRAC7, AtRAC8, and AtRAC10 shows conservation between AtRAC7 Cys-196, AtRAC8 Cys-199, and AtRAC10 Cys-202 and between AtRAC7 Cys-203, AtRAC8 Cys-205, and AtRAC10 Cys-209. AtRAC7 Cys-206 and AtRAC8 Cys-205 are part of the putative CaaX box prenylation motifs (rectangles).

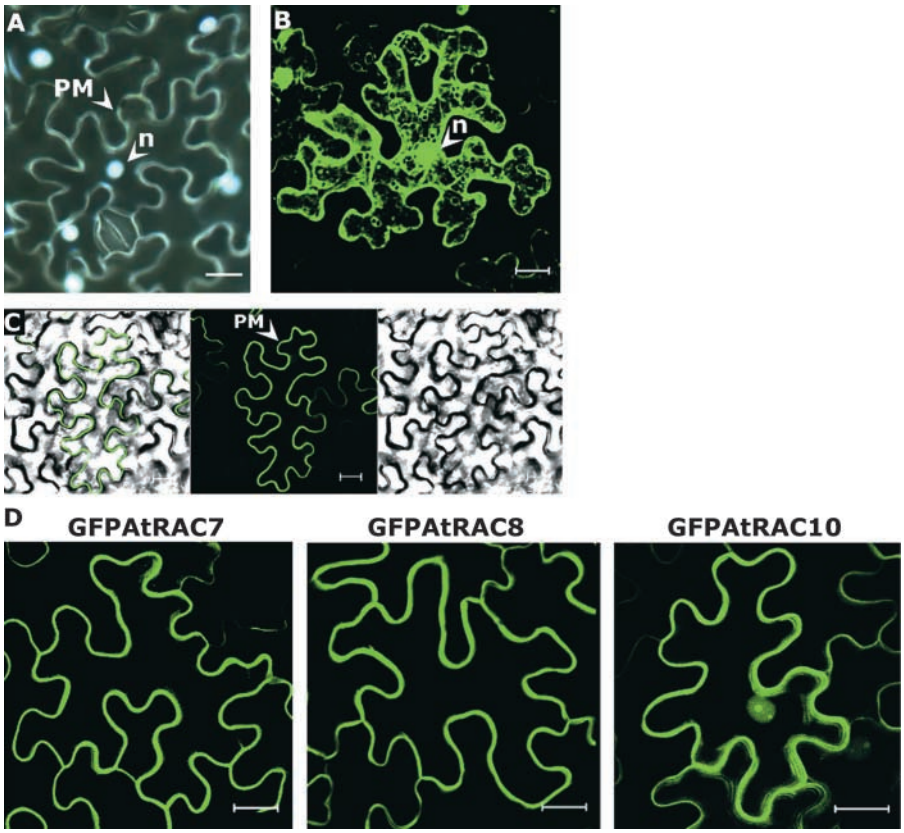

Figure 2. Subcellular Localization of GFP, GFPAtRAC7, GFPAtRAC8, and GFPAtRAC10.

(A) *N. benthamiana* leaf epidermal cells stained with 4′,6-diamidino-2-phenylindole to visualize nuclei (n).
(B) *N. benthamiana* leaf epidermal cell expressing free GFP fluorescence dispersed in the cytoplasm and nuclei (n). GFP does not penetrate vacuoles, which remain unstained. Because of the vacuole size, the cytoplasm often appears as a thick band in the cell periphery. Intracellular staining is caused by cytoplasmic strands.
(C) GFP fluorescence is visualized as a sharp band in the cell periphery of a *N. benthamiana* leaf epidermal cell expressing GFPAtRAC8. At right, Nomarsky differential interference contrast (DIC) image; middle, GFP fluorescence; at left, DIC GFP fluorescence overlay.
(D) *N. benthamiana* leaf epidermal cells expressing GFPAtRAC7, GFPAtRAC8, and GFPAtRAC10. GFP fluorescence appears as a band around the cell periphery. GFPAtRAC10 also is detected in the nuclei.
Cells were visualized with a wide-field fluorescence microscope **(A)** or with a confocal laser scanning microscope (**[B]** to **[D]**). Images in **(D)** are from a projection stack of multiple confocal sections along the *z* axis. PM, plasma membrane. Bars = 20 μm.

found together in membranes and in the cytoplasm. To discover whether AtRAC7, AtRAC8, and AtRAC10 represent a unique case of subcellular distribution, we examined the subcellular localization of a different RAC protein.

RacU88402 (RacU), a Rac protein of unknown function, terminates in a CLLM CaaX box prenylation motif. In vitro prenylation assays were performed to determine whether RacU is prenylated (Figure 3A). In these assays, recombinant His_6-tagged RacU and ^{3}H-farnesyldiphosphate were used as protein and prenyl substrates, respectively, together with recombinant purified FTase (Caldelari et al., 2001). The radiolabeled band shown in Figure 3A indicates that the recombinant RacU was farnesylated in vitro. Prenylation of GFPRacU was tested in yeast cells (Figure 3B). The wild-type GFPRacU was localized in the plasma and internal membranes (Figure 3B, RacU), whereas a mutant protein in which the prenyl acceptor Cys had been changed to Ser (GFPRacUmS^{266}) was dispersed in the cytoplasm (Figure 3B, racUmS^{266}). These results establish a direct causal relationship between prenylation and the subcellular distribution of the GFPRacU fusion protein. After transient expression in *N. benthamiana*, GFPRacU was distributed between the cell membranes and the cytoplasm (Figure 3C). Fluorescence was seen around the cells, in cytoplasmic strings that crossed the cells, and

around the nuclei. Such perinuclear staining often is characteristic of endoplasmic reticulum–localized proteins, suggesting that a fraction of GFPRacU is localized in the endoplasmic reticulum. The apparent difference in subcellular localization between RacU and AtRAC7, AtRAC8, and AtRAC10 or free GFP suggests that the subcellular targeting of prenylated RacU occurs via a different mechanism compared with that seen in type II Rops/RACs.

The Role of the C-Terminal Cys Residues

Differences in subcellular localization between RacU and AtRAC7, AtRAC8, and AtRAC10 prompted us to examine the role of C-terminal Cys residues in membrane association for the three proteins. To this end, site-specific mutants, in which Cys residues were mutated to Ser residues, were created. Mutants are designated with the suffix mS (mutant Ser) based on the location of the corresponding mutated Cys (Figure 4). The following mutants were created: Atrac7mS^{206}, Atrac7mS^{203}, Atrac7mS^{196}, Atrac7mSS$^{203+206}$, Atrac8mS^{205}, Atrac8mS^{199}, Atrac8mSS$^{199+205}$, Atrac10mS^{208}, Atrac10mS^{202}, and Atrac10mSS$^{202+208}$.

All mutants, both single (mS) and double (mSS), were mislocalized from the plasma membrane to the cytoplasm and nucleus (Figure 4). The expression of GFPAtRAC7, GFPAtRAC8, and GFPAtRAC10 was observed as thin bands of fluorescence around the cells (Figures 2D, 4A, 4F, and 4J). When the mS or the mSS mutants were expressed, strings of GFP fluorescence crossed the cells and fluorescing nuclei appeared, indicating cytoplasmic or nuclear localization, respectively (Figures 4B to 4E, 4G to 4I, and 4K to 4M). These results suggest that the C-terminal Cys residues (AtRAC7, Cys-206, Cys-203, and Cys-196; AtRAC8, Cys-205 and Cys-199; and AtRAC10, Cys-208 and Cys-202) act cooperatively to assist the association with the membrane.

Interestingly, mutating the CaaX box Cys of AtRAC7 (Cys-206) had the least effect on the association with the membrane (cf. Figures 4B with 4C and 4E), suggesting that if AtRAC7 is prenylated on Cys-206, prenylation is not obligatory for its association with the plasma membrane. AtRAC7 Cys-196 and Cys-203 were found to align with AtRAC8 Cys-199 and Cys-205 and AtRAC10 Cys-202 and Cys-208 (Figure 1). The results suggest that a domain consisting of two or more Cys residues determines the membrane association of AtRAC7, AtRAC8, and AtRAC10 and that the association with membranes does not require a functional CaaX box. Additional experiments supported this conclusion.

Cells expressing GFPAtRAC7, GFPAtRAC8, and their double-Cys mutants Atrac7mSS$^{203+206}$ and Atrac8m-SS$^{199+205}$ were plasmolyzed to better visualize the subcellular localization of the protein (Figure 5). GFPAtRAC7 and GFPAtRAC8 had typical plasma membrane localization. After plasmolysis, both proteins formed thin fluorescing strands that were attached to the cell wall at only a few points (Figure 5, AtRAC7 and AtRAC8). On the other hand, the double-Cys mutants GFPAtrac7mSS$^{203+206}$ and Atrac8mSS$^{199+205}$ had a typical cytoplasmic distribution, forming regions of

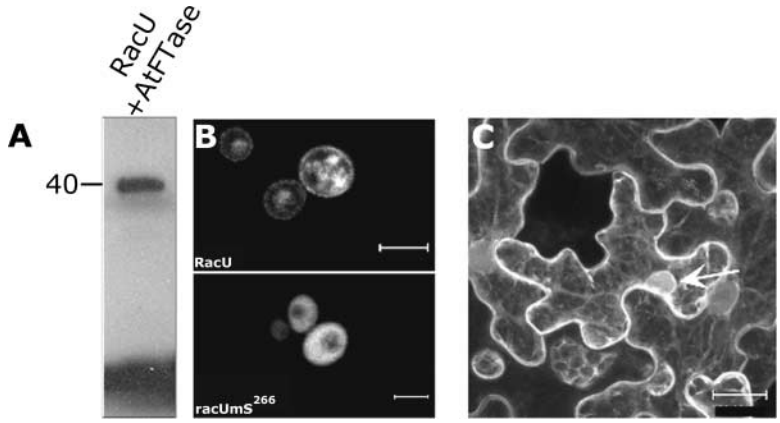

Figure 3. Prenylation and Subcellular Localization of a GFPRacU.

(A) Fluorogram of an SDS-PAGE gel depicting radiolabeled RacU after an in vitro farnesylation assay.
(B) Yeast cells, RacU is localized in the plasma membrane and endomembrane, whereas mutant nonprenylatable GFPracUmS^{266} (racUmS^{266}) is dispersed in the cytoplasm.
(C) After transient expression in a leaf epidermal cell of *N. benthamiana*, GFP-RacU is detected in the plasma membrane, cytoplasmic strands, and around nuclei (arrow). The perinuclear localization is typically to the endoplasmic reticulum.
Images in **(B)** and **(C)** are from projection stacks of multiple confocal scans taken with a confocal laser scanning microscope. Bars = 5 μm in **(B)** and 20 μm in **(C)**.

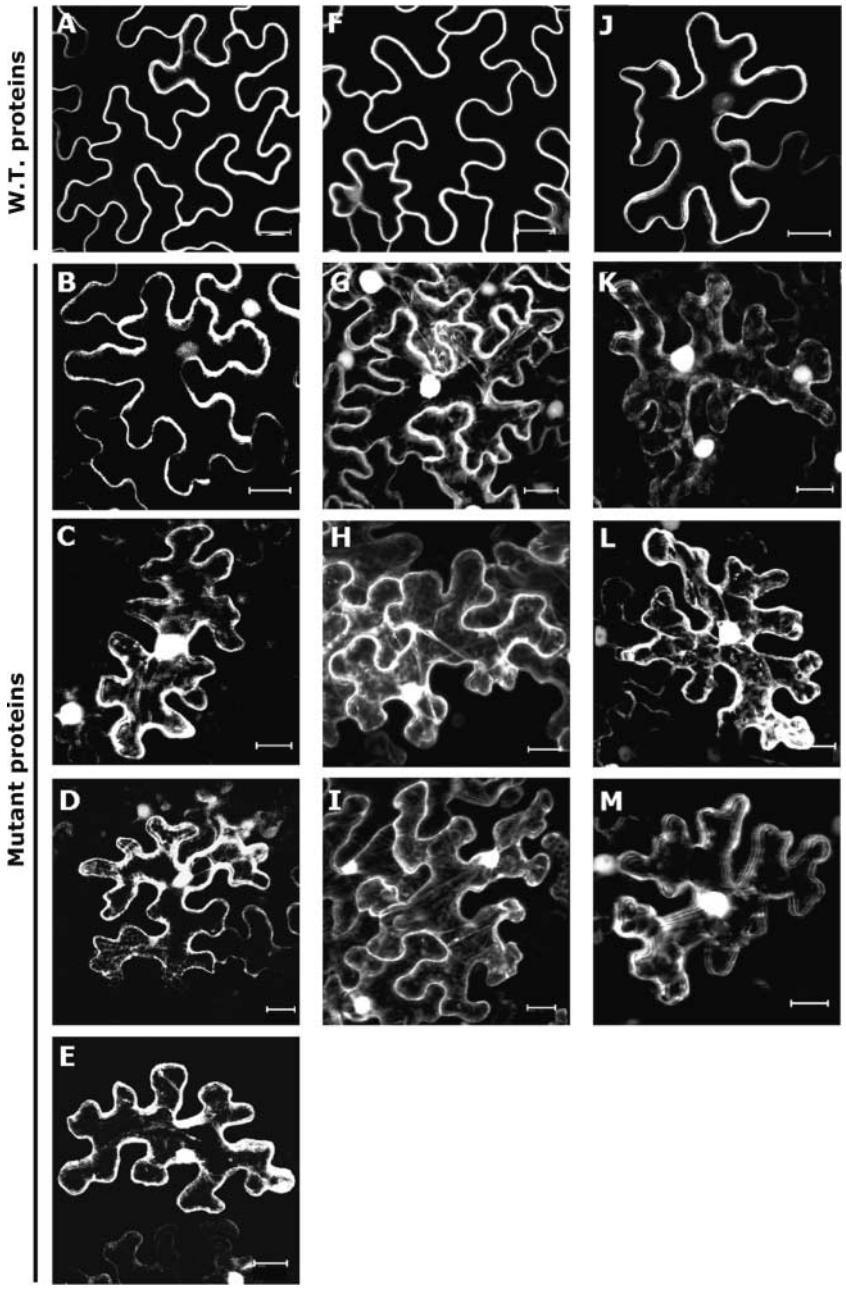

Figure 4. Effect of C-Terminal Cys Residues on the Association of AtRAC7, AtRAC8, and AtRAC10 with Membranes.

Wild-type and mutant GFP-AtRACs were expressed transiently in *N. benthamiana* leaf epidermal cells.
(A) to **(E)** AtRAC7.
(F) to **(I)** AtRAC8.
(J) to **(M)** AtRAC10.
(A), **(F)**, and **(J)** show wild-type proteins. Cys mutants were designated with the suffix mS and received a number specifying the amino acid position. These are shown as follows: Atrac7mS^{206} **(B)**; Atrac7mS^{203} **(C)**; Atrac7mSS$^{203+206}$ **(D)**; Atrac7mS^{196} **(E)**; Atrac8mS^{205} **(G)**; Atrac8mS^{199} **(H)**; Atrac8mSS$^{199+205}$ **(I)**; Atrac10mS^{208} **(K)**; Atrac10mS^{202} **(L)**; and Atrac10mSS$^{202+208}$ **(M)**. Nuclei and cytoplasmic strands were visualized in the Cys mutants, indicating that the association of fusion proteins with the plasma membrane was weaker. Note that with the exception of Atrac7mS^{206}, in which dissociation from the plasma membrane was weaker, mutations in a single Cys were similar in effect to mutations in two Cys residues. All images are from projection stacks of multiple confocal sections taken with a confocal laser scanning microscope. Bars = 20 μm.

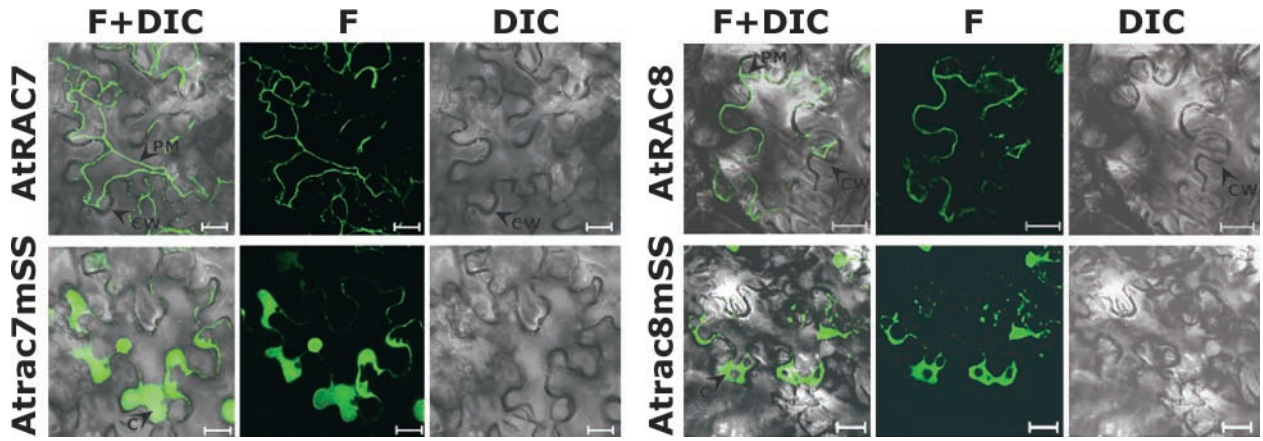

Figure 5. Plasmolysis of *N. benthamiana* Cells Expressing GFPAtRAC7, GFPAtRAC8, and Their Corresponding Double-Cys Mutants.

After plasmolysis, GFP fluorescence was detected in the plasma membrane of cells that expressed GFPAtRAC7 (AtRAC7) or GFPAtRAC8 (AtRAC8). GFP fluorescence had a typical cytoplasmic distribution after plasmolysis of cells that expressed GFPAtrac7mSS$^{203+206}$ (Atrac7mSS) and GFPAtrac8mSS$^{199+205}$ (Atrac8mSS). All images are from confocal scans performed with a confocal laser scanning microscope. DIC, Nomarsky differential interference contrast image; F, GFP fluorescence image; F+DIC, overlay of fluorescence and DIC images. Arrowheads point to the plasma membrane (PM), cytoplasmic thickening (C), and cell walls (CW). Bars = 20 μm.

concentrated fluorescence (Figure 5, Atrac7mSS and Atrac8mSS).

Protein immunoblot analysis using anti-GFP monoclonal antibodies showed that after centrifugal fractionation of cells, GFPAtRAC7 and GFPAtRAC8 were localized in a detergent-soluble pellet, whereas the mutants GFPAtrac7mSS$^{203+206}$ and GFPAtrac8mSS$^{199+205}$ were localized in the water-soluble supernatant (Figure 6). Collectively, the mutant, plasmolysis, and immunoblot analyses (Figures 4 to 6) demonstrated that AtRAC7 and AtRAC8 were localized in the plasma membrane, whereas their cognate double-Cys mutants Atrac7mSS$^{203+206}$ and Atrac8mSS$^{199+205}$ accumulated in the cytoplasm.

A fraction of AtRAC10 was detected in the nucleus (Figures 2 and 4), in contrast to AtRAC7 and AtRAC8, which were detected only in the plasma membrane (Figures 2 and 4 to 6). Plasmolysis was performed to better visualize the subcellular localization of AtRAC10 and Atrac10mSS$^{202+208}$ (Figure 7A). After plasmolysis, GFPAtRAC10 was localized mainly to the plasma membrane, with smaller fractions detected in nuclei and cytoplasm (Figure 7A, AtRAC10). The double-Cys mutant GFPAtrac10mSS$^{202+208}$ was detected primarily in nuclei and cytoplasm (Figure 7A, Atrac10mSS).

Immunoblot analysis was performed to determine whether GFP fluorescence in the cytoplasm and nuclei of cells expressing GFPAtRAC10 could have resulted from partial degradation of the fusion protein and release of the GFP moiety (Figure 7B). Blots of protein extracts from GFPAtRAC10– and free GFP–expressing cells were decorated with anti-GFP antibodies. Only a single band that had a higher molecular mass compared with that of free GFP was detected in the GFPAtRAC10 extract (Figure 7B). These data exclude the possibility that GFP fluorescence in the cytoplasm and nuclei of cells expressing GFPAtRAC10 resulted from degradation of the fusion protein.

To address the possibility that the four amino acid extension was responsible for the different subcellular distribution of AtRAC10 compared with that of AtRAC7 and AtRAC8 (Figure 2D), a mutant of AtRAC8 was created in which the C-terminal four amino acids of AtRAC10 (VTRH) were added to the C-terminal end of AtRAC8 (Atrac8m10C′). GFPAtrac8m10C′ was localized entirely in the plasma membrane, exactly like GFPAtRAC8, and no fluorescing nuclei were detected (Figure 7C). These results indicate that the

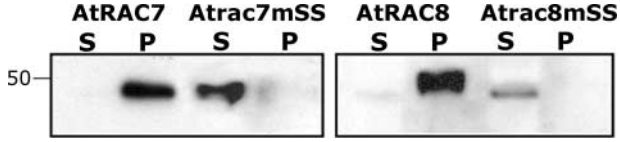

Figure 6. Immunoblot Analysis of Subcellular Fractions Containing AtRAC7, Atrac7mSS$^{203+206}$, AtRAC8, and Atrac8mSS$^{199+205}$.

Detection of GFPAtRAC7 (AtRAC7), GFPAtrac7mSS$^{203+206}$ (Atrac7mSS), GFPAtRAC8 (AtRAC8), and GFPAtrac8mSS$^{199+205}$ (Atrac8mSS) with anti-GFP monoclonal antibodies after transient expression in leaves of *N. benthamiana*, centrifugal separation to soluble (S) and insoluble pellet (P) fractions, and separation by SDS-PAGE. The number at left denotes molecular mass in kD. Note the absence of the double-mutant proteins from the insoluble pellet fraction.

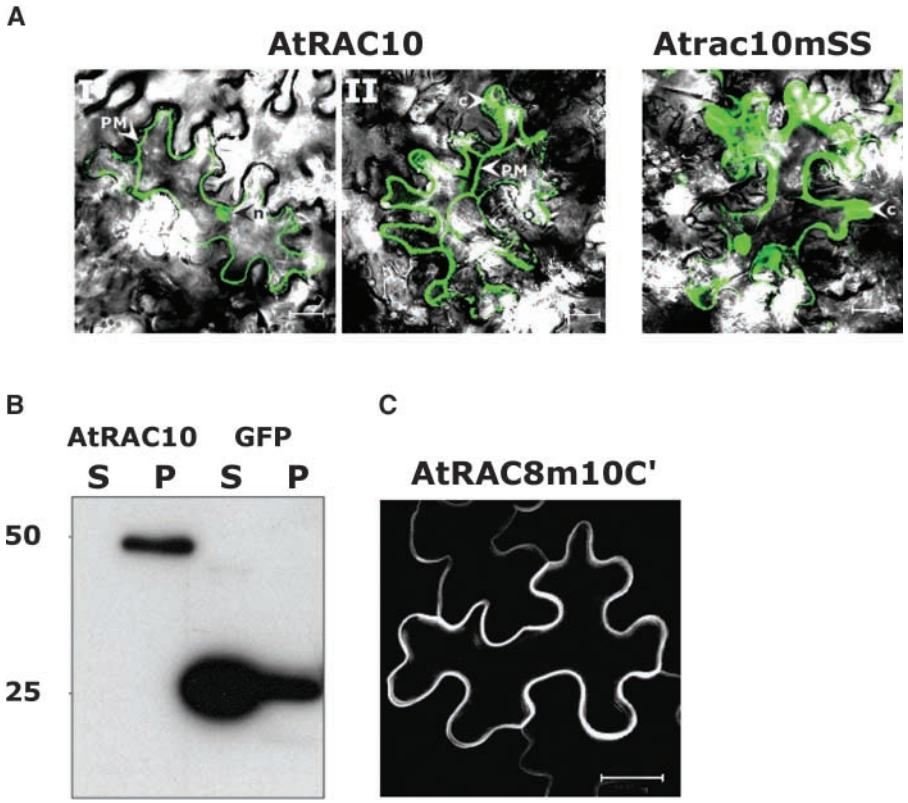

Figure 7. Subcellular Localization of AtRAC10.

(A) *N. benthamiana* leaves that expressed GFPAtRAC10 (AtRAC10) or GFPAtrac10mSS$^{202+208}$ (Atrac10mSS) were plasmolyzed. The majority of the wild-type protein was detected in the plasma membrane (PM), with smaller fractions in nuclei (n) (AtRAC10, I and II). In a few cells, cytoplasmic thickening (C) was detected (AtRAC10, II). The mutant protein (Atrac10mSS) was detected only in nuclei and cytoplasmic thickening.
(B) Immunoblot analysis of a protein with anti-GFP monoclonal antibodies after transient expression of GFPAtRAC10 (AtRAC10) or free GFP (GFP) in leaves of *N. benthamiana*, centrifugal separation to soluble (S) and insoluble pellet (P) fractions, and separation by SDS-PAGE.
(C) A mutant of AtRAC8 containing the four C-terminal residues of AtRAC10 (Atrac8m10C′) was localized only in the plasma membrane, similar to wild-type AtRAC8.
Images in **(A)** are differential interference contrast and fluorescence overlays. All images are confocal scans taken with a confocal laser scanning microscope. Numbers at left in **(B)** denote molecular mass in kD. Bars = 20 μm.

difference between AtRAC8 and AtRAC10 is independent of a C-terminal CXXX motif.

Palmitoylation Assays of AtRAC7, AtRAC8, and AtRAC10

Because the attachment of AtRAC7, AtRAC8, and AtRAC10 to the plasma membrane depends on internal Cys residues (Figure 4), they likely undergo a post-translational modification that is not prenylation. Protein palmitoylation involves attachment of the acyl lipid palmitate to Cys residues by a reversible thioester bond (Linder, 2000). Thus, palmitoylation might be the modification required for the attachment of AtRAC7, AtRAC8, and AtRAC10 to the plasma membrane. No consensus sequences for palmitoylation have been identified. In addition, in vitro, palmitoylation occurs spontaneously and does not depend on additional enzymatic activity (Resh, 1999; Linder, 2000). However, the in vitro palmitoylation reactions require Cys residues with free thiol groups and show sensitivity to palmitoylation inhibitors (Webb et al., 2000; Veit et al., 2001).

In vitro palmitoylation assays were performed to determine whether AtRACs could be palmitoylated (Figure 8). These assays were performed by incubating recombinant AtRAC8 or Atrac8mSS with ^{3}H-palmitoyl-CoA without an additional protein extract. AtRAC8 was labeled after incubation with radiolabeled palmitoyl-CoA (Figure 8, AtRAC8). However, when the palmitoylation inhibitor 2-bromopalmi-

tate (Webb et al., 2000; Michaelson et al., 2001; Veit et al., 2001) was added to the reaction, the labeling of AtRAC8 was reduced substantially (Figure 8, AtRAC8+2-bromopalmitate). No labeling of the double-Cys mutant Atrac8mSS$^{199+205}$ was detected (Figure 8, AtRAC8mSS), demonstrating that the labeling of AtRAC8 is dependent on the C-terminal Cys residues. These data suggested that AtRAC8 is in fact a palmitoylated protein. Furthermore, the amino acid sequence similarity and the similar subcellular localization suggested that AtRAC7 and AtRAC10 probably also are palmitoylated.

To determine whether AtRAC7, AtRAC8, and AtRAC10 are palmitoylated in vivo, GFP fusion versions of all three proteins were expressed in the presence of 2-bromopalmitate. The inhibitor 2-bromopalmitate is used widely to demonstrate protein palmitoylation and its role in subcellular protein targeting (Webb et al., 2000; Michaelson et al., 2001; Veit et al., 2001) (Figure 9). The inhibitor 2-bromopalmitate was applied to leaves together with *Agrobacterium tumefaciens* cells. The presence of 2-bromopalmitate caused mislocalization of the three fusion proteins from plasma membrane to cytoplasm and nuclei (Figure 9), similar to the mS and mSS mutations (Figure 4). Injection of DMSO (the solvent used to dissolve 2-bromopalmitate) alone had no effect on the membrane localization of the GFPAtRACs (Figure 9).

Thus, the association of AtRAC7, AtRAC8, and AtRAC10 with the plasma membrane likely is promoted by their palmitoylation. However, the possibility that AtRAC7 and AtRAC8 are prenylated could not be excluded, and additional experiments were performed to clarify this point.

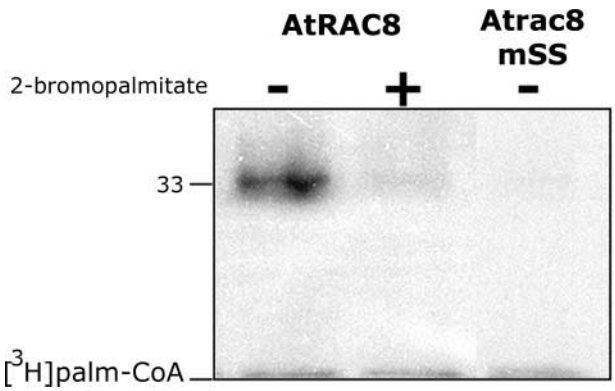

Figure 8. In Vitro Palmitoylation of AtRAC8.

Fluorogram of an in vitro palmitoylation reaction. Recombinant His_6-AtRAC8 (AtRAC8) was palmitoylated after incubation with ^{3}H-palmitoyl-CoA ([^{3}H]palm-CoA). Palmitoylation was reduced substantially in the presence of the palmitoylation inhibitor 2-bromopalmitate (+). Similarly, the double-Cys mutant (Atrac8mSS), which lacked the palmitate acceptor Cys residues, was not labeled. The number at left denotes molecular mass in kD.

Prenylation Assays of AtRAC7 and AtRAC8

A direct causal relationship between prenylation and subcellular localization in yeast was established for RacU (Figure 3). Similarly, in vivo prenylation assays for GFP-RACs were established using strains of the *ram1Δ* mutant of *S. cerevisiae* (in which *RAM1*, the gene encoding the FTase β-subunit, was knocked out), which coexpressed the α- and β-subunits of a plant FTase (Yalovsky et al., 1997) or GGTase-I (Figure 10).

GFPAtRAC7 was localized in the plasma membrane in cells that expressed either LeFTase or AtGGTase-I (Figure 10, AtRAC7, *ram1Δ*+LeFTase or *ram1Δ*+AtGGTase-I), but it was dispersed in the cytoplasm in mutant *ram1Δ* cells that did not express either of the two prenyltransferases (Figure 10, AtRAC7, *ram1Δ*). Mutant Atrac7mS^{206} (in which the prenyl acceptor Cys was mutated to Ser) was dispersed in the cytoplasm regardless of the presence of either prenyltransferase (Figure 10, Atrac7mS^{206}). In contrast to GFPAtRAC7, GFPAtRAC8 was dispersed in the cytoplasm regardless of the presence of the plant FTase or GGTase-I (Figure 10, AtRAC8 and Atrac8mS^{205}). These data demonstrate that in *S. cerevisiae*, GFPAtRAC7 is a substrate of FTase and GGTase-I, but GFPAtRAC8 is likely not prenylated. Indeed, in vitro assays failed to demonstrate the prenylation of AtRAC8 (data not shown).

To assess whether the membrane localization of GFPAtRAC7 and GFPAtRAC8 depends on FTase in plants, both proteins were expressed in leaves of Arabidopsis *era1-2* mutant plants, in which the single gene encoding the FTase β-subunit had been deleted (Cutler et al., 1996) (Figure 11A). The results show that the membrane association of both AtRAC7 and AtRAC8 was independent of farnesylation. In both *era1-2* and wild-type plants, both GFPAtRAC7 and GFPAtRAC8 were localized to the plasma membranes (Figure 11A, wild type versus *era1-2*).

Prenylation by GGTase-I (Figure 10) still could account for the plasma membrane association of GFPAtRAC7 in *era1-2*. To examine further whether prenylation is involved in the association of AtRAC7 and AtRAC8 with the plasma membranes, we created mutants of both proteins that terminate prematurely, lacking their last residue (Atrac7mCaa− and Atrac8mCaa−). These mutants contain C-terminal CTA and CGK sequence motifs instead of CTAA and CGKN CaaX boxes, respectively. In *N. benthamiana*, GFPAtrac7mCaa− and GFPAtrac8mCaa− were localized in the plasma membrane, exactly like their corresponding wild-type proteins (Figure 11B). This finding further establishes that prenylation is not required for the association of AtRAC7 and AtRAC8 with the plasma membrane of plant cells. However, it should be noted that we cannot exclude the prenylation of AtRAC7 under specific conditions.

Together, our results suggest that AtRAC7, AtRAC8, and

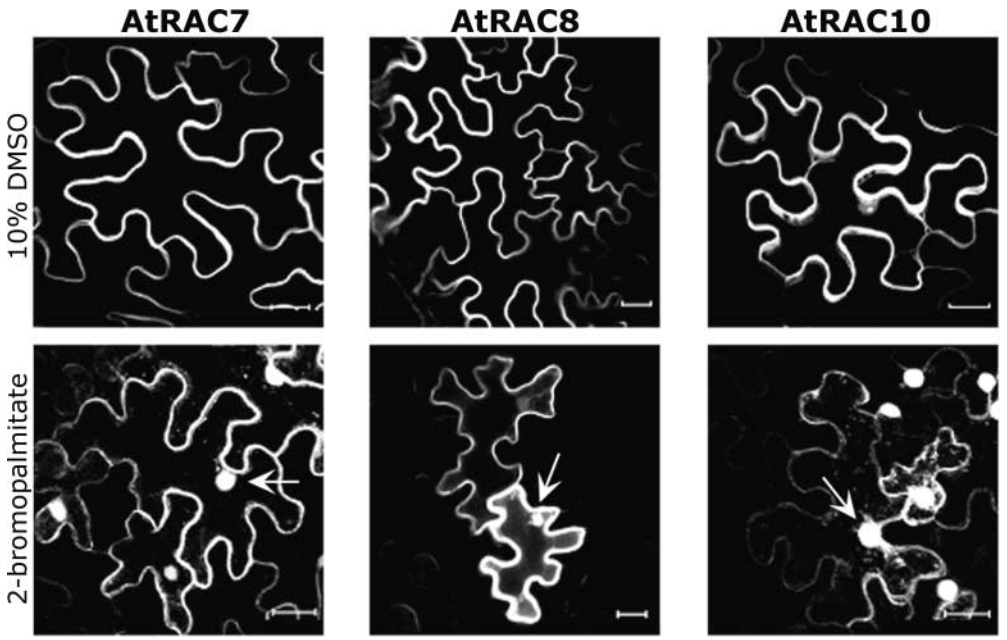

Figure 9. Inhibition of Protein Palmitoylation Released AtRAC7, AtRAC8, and AtRAC10 from Plasma Membrane.

Nuclei (arrow) and cytoplasmic strands could be visualized when GFPAtRAC7, GFPAtRAC8, and GFPAtRAC10 were expressed transiently in leaves of *N. benthamiana* in the presence of 2-bromopalmitate, demonstrating that palmitoylation is required for the association of the three AtRACs with the plasma membrane (2-bromopalmitate). Injection of DMSO alone (10% DMSO) did not affect the ability of the protein to associate with the plasma membrane. The images are from projection stacks of multiple confocal sections taken with a confocal laser scanning microscope. Bars = 20 μm.

AtRAC10 are targeted to the plasma membrane by a plant-unique mechanism (differing from the situation in yeast) that likely involves the palmitoylation of Cys residues at the hypervariable C-terminal end of the proteins.

Cell-Specific Mechanism Involved in Targeting AtRAC7 and AtRAC8

As shown above, AtRAC7, AtRAC8, and AtRAC10 likely are palmitoylated, but not prenylated, whereas type I Rops/RACs are prenylated (Lin et al., 1996; Trainin et al., 1996). In animal cells, researchers have used artificial myristoylated forms of H-Ras to determine whether this protein must be prenylated to exert its biological activity (Buss et al., 1989; Willumsen et al., 1996). Compared with the animal system, the plant type I and II Rops/RACs enable examination of the same questions without having to use artificial protein forms.

Arabidopsis Rop4At and Rop6At localize in a polar manner inside dividing and elongating cells. Both Rop4At and Rop6At accumulated in the cell plates of dividing BY-2 cells, in the transverse membranes of dividing and growing root cells, and at the tips of growing root hairs (Molendijk et al., 2001). Similarly, Arabidopsis Rop1At and Rop2At were found at the tips of growing pollen tube and root hair cells, respectively (Lin et al., 1996; Jones et al., 2002). The polar localization of Rop proteins in root hair and pollen tube cells coincides with the establishment of Ca^{2+} gradients and the distribution of actin filaments (Zheng and Yang, 2000b; Fu et al., 2001; Molendijk et al., 2001).

Transgenic Arabidopsis lines expressing GFPAtRAC8 and GFPAtrac7mV[15] were created, and the localization of the fusion proteins in different cells types and tissues was examined (Figures 12 and 13). Changing a Gly residue, conserved throughout all small GTP binding proteins, to Val created Atrac7mV[15]. This change causes the protein to become constitutively active (Zheng and Yang, 2000b; Fu et al., 2001; Molendijk et al., 2001). Figures 12A, 12B, and 12D show a region of the root tip. GFP fluorescence was distributed evenly around the cells in the area of the meristem (Figure 12A) and in elongating cells located just above the meristem (Figures 12A [the black rectangle], 12B, and 12D).

A second example of dividing cells was the developing guard cells of stomata (Figures 12C and 12E). Guard cells develop through a series of tightly regulated polar asymmet-

ric cell divisions (Sachs, 1991; Larkin et al., 1997). Again, as in the developing root, GFPAtRAC8 and GFPAtrac7mV[15] were distributed evenly around the cells (Figures 12C and 12E), indicating that its localization did not coincide with the polar orientation of the plane of cell division.

In root hairs, the localization of Rop4At, Rop6At, and Rop2At at the tip is required for cell elongation (Molendijk et al., 2001; Jones et al., 2002). In the same cells, GFPAtrac7mV[15] and GFPAtRAC8 were not localized in the membrane at all (Figure 13), providing evidence that the mechanism that promotes the attachment of these proteins to the plasma membrane does not exist in root hairs. These results provide evidence that the targeting of AtRAC7 and AtRAC8 (and probably of AtRAC10 as well) to the plasma membrane occurs by a plant cell–specific mechanism. Ectopic expression of the constitutively active mutant GFPAtrac7mV[15] did not induce the deformation of root hair cells (Figure 13B), contrary to the effect of constitutively active rop4At, rop6At, and rop2At mutants. These results suggest that type II Rops/RACs may not be involved in the establishment of cell polarity in root hairs.

DISCUSSION

The interplay between the association with membranes and the interaction with RHO·GDIs is pivotal in the regulation of RHO GTPases (Olofsson, 1999). Prenylation promotes both the association of RHO GTPases with cell membranes and their interaction with RHO·GDIs (Hall, 1998; Olofsson, 1999). Postprenylation palmitoylation has been shown to inhibit the interaction between Rho and RHO·GDIs (Michaelson et al., 2001). Thus, AtRAC7, AtRAC8, and AtRAC10 may be subject to a unique mode of regulation because they are likely palmitoylated, but not prenylated, or in the case of AtRAC7, they may be prenylated under specific conditions.

Prenylated RHOs were found in the cytoplasm as well as in the membrane (Figure 3C) (Ivanchenko et al., 2000; Molendijk et al., 2001). By contrast, GFPAtRAC7 and GFPAtRAC8 were not found in the cytoplasm, suggesting that they did not associate with cytoplasmic factors. A small fraction of GFPAtRAC10 was found in the cytoplasm

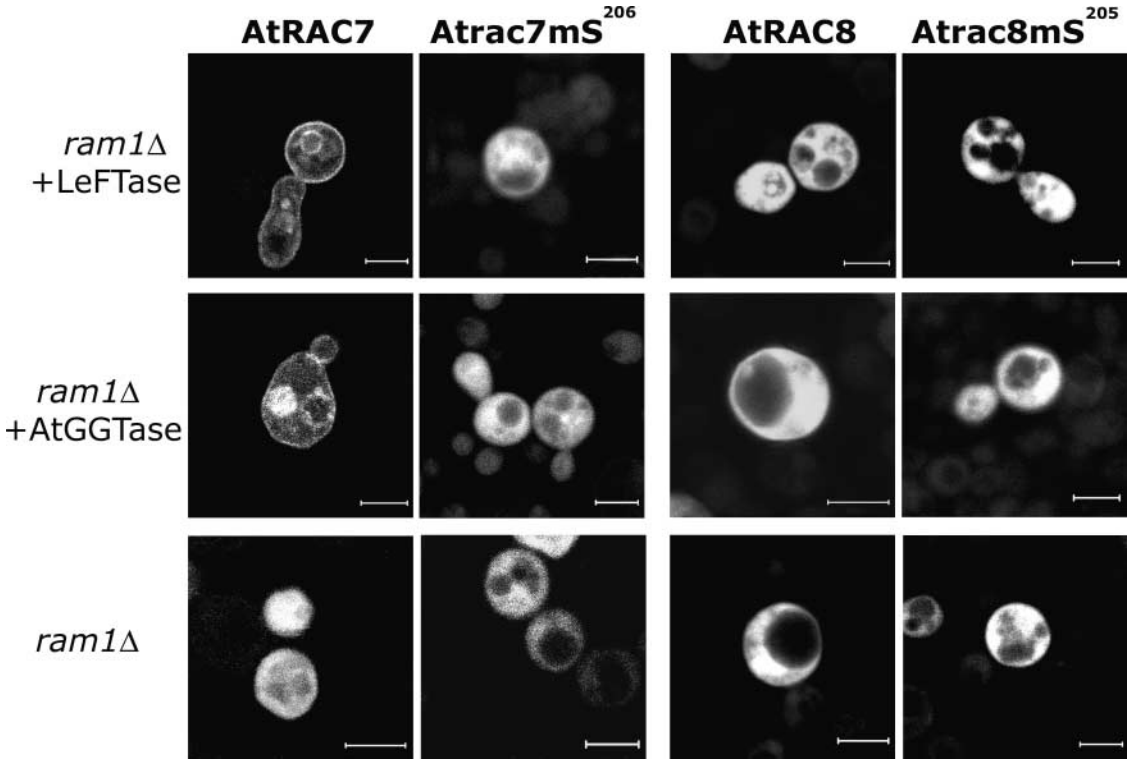

Figure 10. Prenylation Assays of GFPAtRAC7 and GFPAtRAC8 in *S. cerevisiae*.

GFPAtRAC7 was associated with membranes when coexpressed together with the α- and β-subunits of tomato FTase (LeFTase) or Arabidopsis GGTase-I (AtGGTase) in *ram1Δ* yeast cells in which the β-subunit of yeast FTase had been deleted. In the absence of either prenyltransferase (*ram1Δ*), GFPAtRAC7 was dispersed in the cytoplasm. In contrast to GFPAtRAC7, GFPAtrac7mS[206], GFPAtRAC8, and GFPAtrac8mS[205] were dispersed in the cytoplasm regardless of the presence of either LeFTase or AtGGT-I. Bars = 5 μm.

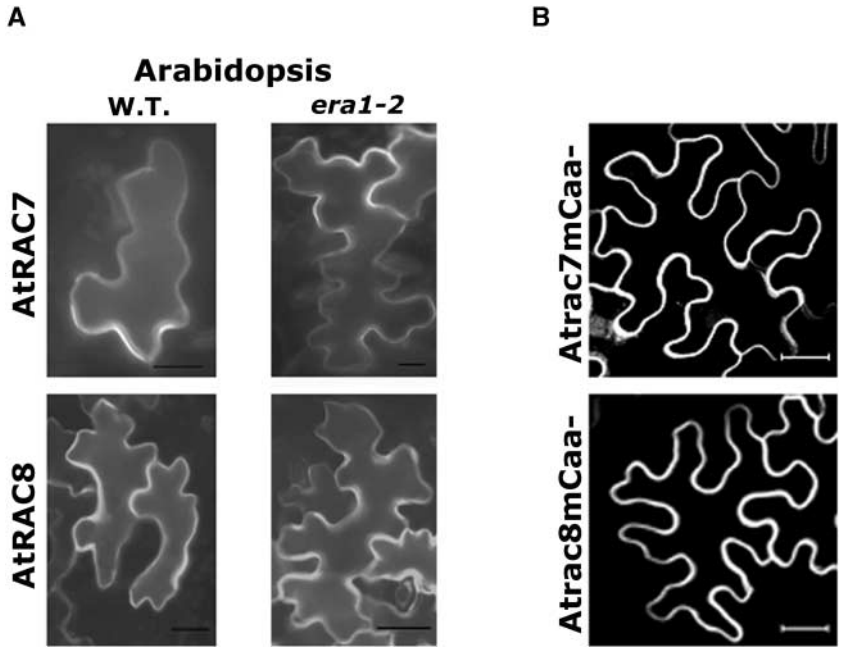

Figure 11. Subcellular Localization of AtRAC7 and AtRAC8 in Plant Cells in the Absence of FTase or a Functional CaaX Box.

Neither FTase nor a functional CaaX box was required for the association of AtRAC7 and AtRAC8 with the plasma membrane.
(A) GFPAtRAC7 and GFPAtRAC8 were associated with the membranes when expressed transiently in leaf epidermal cells of either wild-type (W.T.) or *era1-2* mutant Arabidopsis in which the β-subunit of FTase had been deleted.
(B) GFPAtrac7mCaa− (Atrac7mCaa−) and GFPAtrac8mCaa− (Atrac8mCaa−), in which the last amino acid was deleted, were associated with the plasma membrane after transient expression in *N. benthamiana* leaf epidermal cells.
Images were acquired using a wide-field fluorescence microscope **(A)** or a confocal laser scanning microscope **(B)**. Images in **(B)** are from projection stacks of multiple confocal scans. Bars = 20 μm.

and the nucleus; thus, this protein could interact with proteins in these cell fractions. It is noteworthy that the nuclear localization of lipid-unmodified proteins results from the C-terminal polybasic domains, which in plants serve as a nuclear localization signal (Rodriguez-Concepcion et al., 1999b).

Palmitoylation status may regulate AtRAC7, AtRAC8, and AtRAC10. Such regulation is exemplified in Atrac7mV[15] and AtRAC8, which were not associated with the plasma membrane in the root hair cell (Figure 13). Palmitoylation is a reversible modification, and certain palmitoylated proteins, such as some α-subunits of trimeric G-proteins (Mumby et al., 1994; Wedegaertner and Bourne, 1994), nitric oxide synthase (Feron et al., 1998; Yeh et al., 1999), and certain Tyr protein kinases (Wolven et al., 1997), undergo regulated cycles of palmitoylation and depalmitoylation (for reviews, see Mumby, 1997; Resh, 1999; Linder, 2000). The question arises of whether AtRAC7, AtRAC8, and AtRAC10 undergo similar cycles of palmitoylation and depalmitoylation.

Although AtRAC7 is prenylated in yeast, in plants its association with the plasma membrane is prenylation independent (Figures 4 and 9 to 11). Yet, the prenylation of AtRAC7 in plants cannot be excluded and might have an important regulatory role.

There is an ongoing debate regarding whether protein palmitoylation is regulated biologically, because in vitro it occurs in the absence of additional enzymatic activity (Linder, 2000). The apparent differences between the plant and yeast systems suggest that there must be an active biological mechanism that promotes the palmitoylation and membrane targeting of AtRAC7, AtRAC8, and AtRAC10. This finding is supported further by the fact that in root hair cells, AtRAC8 and Atrac7mV[15] were not associated with the plasma membrane (Figure 13).

Because *S. cerevisiae* lacks some of the components required to target AtRAC7, AtRAC8, and AtRAC10 to the plasma membrane, the yeast system provides a powerful tool for studying the function of individual plant genes. *S. cerevisiae* cells could be used to screen for plant genes that promote the association of type II Rop/RAC GTPases with the plasma membrane. Such screening would not require the use of a specific mutant strain of yeast. The yeast system also provides a tool for testing the activity of genes isolated by other means.

Type I Arabidopsis Rop/RAC GTPases are involved in regulating polar cell division and elongation (Li et al., 1999; Fu et al., 2001, 2002; Molendijk et al., 2001; Jones et al., 2002). By contrast, the subcellular localization of AtRAC8 and Atrac7mV[15] within dividing and elongating cells is not polar (Figure 12). Moreover, the constitutively active mutant Atrac7mV[15] does not induce the deformation of root hair cells (Figure 13), unlike its prenylated homologs (Molendijk et al., 2001; Jones et al., 2002).

Recently, it was shown that palmitoylated proteins partition into sphingolipid- and sterol-rich membrane domains termed lipid rafts (Zacharias et al., 2002). The same study showed that prenylated proteins are excluded from lipid rafts. The existence of lipid rafts in membranes of plant cells has been demonstrated (Peskan et al., 2000; Xu et al., 2001). It would be of interest to determine whether prenylated Rops/RACs and type II RACs partition into different membrane domains, thereby acting in different signaling cascades.

Like Ras proteins in yeast and animal cells, AtRAC7, AtRAC8, and AtRAC10 were found primarily in the plasma membrane. The plant type II Rops/RACs might be involved in transmembrane, receptor-mediated signal transduction, thus providing the equivalent of Ras proteins, which are absent in plants. Interestingly, anti-Rop polyclonal antibodies identified a Rop/RAC protein that copurified with the CLAVATA1 protein kinase receptor complex (Trotochaud et al., 1999). It remains unknown whether this Rop is type I or type II.

The combination of yeast and plant mutants has enabled us to identify a plant-unique mechanism that targets type II Rop/RAC GTPases to the plasma membrane. This mechanism most likely prevents the potential prenylation of the GTPase and likely involves the palmitoylation

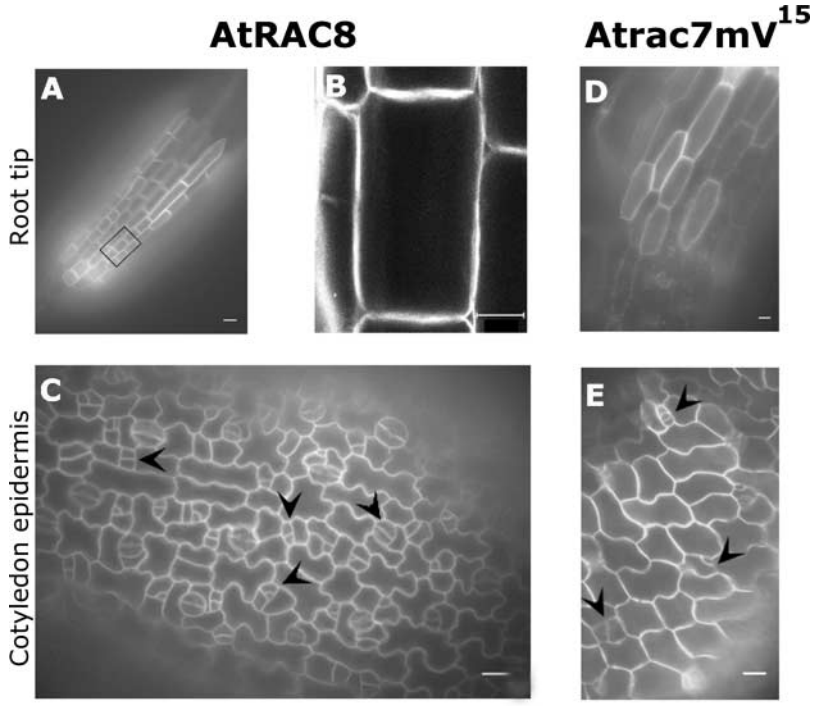

Figure 12. Subcellular Localization of GFPAtRAC8 and GFPAtRAC7mV[15] in Dividing and Elongating Cells.

Both GFPAtRAC8 and GFPAtrac7mV[15] were distributed evenly around the cell periphery in dividing and elongating root cells (**[A]**, **[B]**, and **[D]**) and in developing stomata guard cells (**[C]** and **[E]**).

(A) Region of the root tip of a transgenic Arabidopsis plant expressing GFPAtRAC8.

(B) The black rectangle denotes the cell that was observed in detail with the confocal laser scanning microscope. This image is from a projection stack of multiple confocal sections.

(C) Unequal cell divisions (arrowheads) leading to the development of stomata guard cells can be viewed in the cotyledon epidermis of the same transgenic plant shown in **(A)** and **(B)**.

(D) Elongating root cells from a GFPAtracmV[15]-expressing plant.

(E) Cotyledon epidermis of the same plant shown in **(D)**. Arrowheads point to developing stomata guard cells.

Images in **(A)**, **(C)**, **(D)**, and **(E)** were taken with a wide-field fluorescence microscope. Bars = 20 μm.

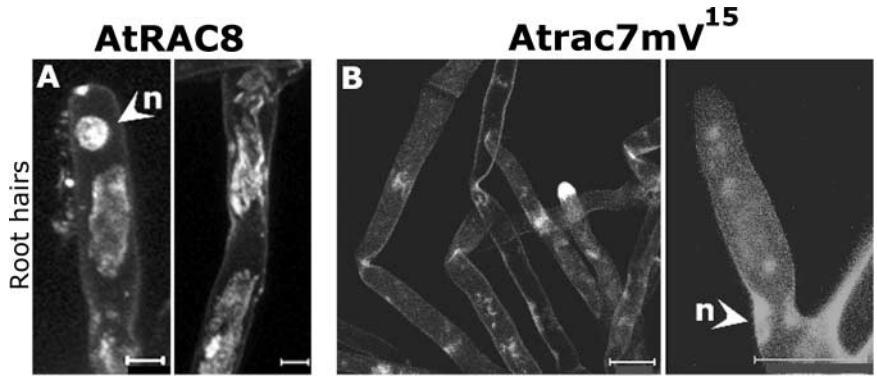

Figure 13. Subcellular Localization of GFPAtRAC8 and GFPAtrac7mV^{15} in Root Hair Cells.

GFPAtRAC8 **(A)** and the constitutively active mutant GFPAtrac7mV^{15} **(B)** were not localized in the plasma membrane of the root hair cells. Interestingly, root hairs that overexpressed GFPAtrac7mV^{15} were not deformed. Images are from projection stacks of multiple confocal scans taken with a confocal laser scanning microscope. Root hair cells were taken from independent transgenic lines that showed the same distribution of GFPAtRAC8 and GFPAtrac7mV^{15}. n, nuclei. Bars = 20 μm.

of two or more C-terminal Cys residues. Palmitoylation and the lack of prenylation suggest that AtRAC7, AtRAC8, and AtRAC10 may not interact with RHO·GDIs, which are key regulators for all other known RHOs. In root hair cells, GFPAtRAC8 and GFPAtrac7mV^{15} were not found in the membrane, whereas prenylated Arabidopsis Rops/RACs are membrane bound and required for the polar elongation of these cells. Moreover, the constitutively active mutant GFPAtrac7mV^{15} failed to induce root hair cell deformation. Thus, AtRAC7, AtRAC8, and AtRAC10 may represent a group of proteins that have evolved to function in unique signaling cascades.

METHODS

Cloning

All plasmids are listed in Table 1. Plasmid numbers refer to the numbering in Table 1. *AtRAC7*, *AtRAC8*, and *AtRAC10* were amplified by PCR from a flower cDNA library using primer pairs as indicated in Tables 2 and 3. *RAC-U88402* (*RacU*) is an EST clone obtained from the ABRC (Columbus, OH). All four genes were subcloned to pGEM (Promega) to create plasmids 2 to 5 (Table 1). Cloning procedures were performed using *Escherichia coli* strains DH5α and JM109.

Site-Directed Mutagenesis

Site-directed mutagenesis was performed using (1) direct PCR, (2) sequential PCR steps (Ausubel et al., 1995), or (3) the QuikChange kit (Stratagene). Primers are listed in Table 2. Mutants and mutagenesis methods are listed in Table 3. ExTaq DNA polymerase (Takara, Otsu, Japan) was used in all reactions. All clones were sequenced to verify that no PCR-generated errors had been introduced.

Plant Expression Plasmids

To express green fluorescent protein (GFP)–AtRAC fusion proteins, fragments containing wild-type and mutant genes were digested with SacI and XbaI (apart from plasmids 3 and 18, which were digested with SacI) and subcloned in frame into pGFP-MRC to create plasmids 20 to 38. For expression in plants, all pGFP-MRC-AtRAC plasmids were digested using HindIII; the resulting cassettes, containing the 35S promoter of *Cauliflower mosaic virus*, the gene of interest, and the nitric oxide synthase transcriptional terminator, were subcloned into pCAMBIA 2300 (CAMBIA, Canberra, Australia) to create plasmids 40 to 58.

Plant Material

Nicotiana benthamiana plants were grown in 10-cm pots. Seeds were sown on soil (Avi Saddeh mix; Pecka Hipper Gan, Rehovot, Israel). Plants were grown under long-day conditions (16-h-light/8-h-dark cycles) at 27°C. The light intensity was 100 $\mu E \cdot m^{-2} \cdot s^{-1}$. Wild-type Columbia and mutant *era1-2 Arabidopsis thaliana* plants were grown in 5-cm pots. Plants were grown on soil (Avi Saddeh mix) and irrigated from below. Plants were grown under long-day conditions (16-h-light/8-h-dark cycles) at 23°C. The light intensity was 100 $\mu E \cdot m^{-2} \cdot s^{-1}$.

Leaf Injections

Leaves from *N. benthamiana* and Arabidopsis were injected with *Agrobacterium tumefaciens* strains GV3101/mp90 harboring the ap-

Table 1. Plasmids Used in This Study

No.	Plasmid Name	Description	Source or Reference
1	pGEM	PCR product TA cloning vector, ampicillin resistant	Promega
2	pSY125	*pGEM-AtRAC7*	This study
3	pSY104	*pGEM-AtRAC8*	This study
4	pSY118	*pGEM-AtRAC10*	This study
5	pSY106	*pGEM-RacU*	This study
6	pSY126	*pGEM-Atrac7mS*^{206}	This study
7	pSY105	*pGEM-Atrac8mS*^{205}	This study
8	pSY155	*pGEM-Atrac10mS*^{208}	This study
9	pSY107	*pGEM-racUmS*^{266}	This study
10	pSY145	*pGEM-Atrac7mS*^{203}	This study
11	pSY157	*pGEM-Atrac8mS*^{199}	This study
12	pSY141	*pGEM-Atrac10mS*^{202}	This study
13	pSY143	*pGEM-Atrac7mSS*$^{203+206}$	This study
14	pSY122	*pGEM-Atrac8mSS*$^{199+205}$	This study
15	pSY120	*pGEM-Atrac10mSS*$^{202+208}$	This study
16	pSY149	*pGEM-Atrac7mCaa*$^{-}$	This study
17	pSY139	*pGEM-Atracm8Caa*$^{-}$	This study
18	pSY147	*pGEM-Atrac8m10C′*	This study
19	pGFP-MRC	35S::GFP-NOS 3′ end, ampicillin resistant	Rodriguez-Concepcion et al., 1999b
20	pSY127	*pGFP-MRC-AtRAC7*	This study
21	pSY108	*pGFP-MRC-AtRAC8*	This study
22	pSY119	*pGFP-MRC-AtRAC10*	This study
23	pSY110	*pGFP-MRC-RacU*	This study
24	pSY128	*pGFP-MRC-Atrac7mS*^{206}	This study
25	pSY109	*pGFP-MRC-Atrac8mS*^{205}	This study
26	pSY156	*pGFP-MRC-Atrac10mS*^{208}	This study
27	pSY99	*pGFP-MRC-racUmS*^{266}	This study
28	pSY146	*pGFP-MRC-Atrac7mS*^{203}	This study
29	pSY164	*pGFP-MRC-Atrac7mS*^{196}	This study
30	pSY124	*pGFP-MRC-Atrac8mS*^{199}	This study
31	pSY142	*pGFP-MRC-Atrac10mS*^{202}	This study
32	pSY144	*pGFP-MRC-Atrac7mSS*$^{203+206}$	This study
33	pSY123	*pGFP-MRC-Atrac8mSS*$^{199+205}$	This study
34	pSY121	*pGFP-MRC-Atrac10mSS*$^{202+208}$	This study
35	pSY159	*pGFP-MRC-Atrac7mCaa*$^{-}$	This study
36	pSY140	*pGFP-MRC-Atracm8Caa*$^{-}$	This study
37	pSY148	*pGFP-MRC-Atrac8m10C′*	This study
38	pSY166	*pGFP-MRC-Atrac7mV*^{15}	This study
39	pCAMBIA 2300	Plant TDNA-based binary vector, kanamycin resistant	CAMBIA
40	pSY56	*pCAMBIA 2300-GFP*	This study
41	pSY130	*pCAMBIA 2300-GFPAtRAC7*	This study
42	pSY115	*pCAMBIA 2300-GFPAtRAC8*	This study
43	pSY132	*pCAMBIA 2300-GFPAtRAC10*	This study
44	pSY117	*pCAMBIA 2300-GFPRACU*	This study
45	pSY131	*pCAMBIA 2300-GFPAtrac7mS*^{206}	This study
46	pSY116	*pCAMBIA 2300-GFPAtrac8mS*^{205}	This study
47	pSY135	*pCAMBIA 2300-GFPAtrac10mS*^{208}	This study
48	pSY153	*pCAMBIA 2300-GFPAtrac7mS*^{203}	This study
49	pSY165	*pCAMBIA 2300-GFPAtrac7mS*^{196}	This study
50	pSY134	*pCAMBIA 2300-GFPAtrac8mS*^{199}	This study
51	pSY151	*pCAMBIA 2300-GFPAtrac10mS*^{202}	This study
52	pSY152	*pCAMBIA 2300-GFPAtrac7mSS*$^{203+206}$	This study
53	pSY136	*pCAMBIA 2300-GFPAtrac8mSS*$^{199+205}$	This study
54	pSY133	*pCAMBIA 2300-GFPAtrac10mSS*$^{202+208}$	This study
55	pSY160	*pCAMBIA 2300-GFPAtrac7mCaa*$^{-}$	This study
56	pSY150	*pCAMBIA 2300-GFPAtracm8Caa*$^{-}$	This study
57	pSY154	*pCAMBIA 2300-GFPAtrac8m10C′*	This study
58	pSY169	*pCAMBIA 2300-GFPAtrac7mV*^{15}	This study
59	pJR1138	Yeast high-copy 2μ shuttle vector	Yalovsky et al., 1997
60	pSY32	*pJR1138-GFPAtRAC7*	This study
61	pSY33	*pJR1138-GFPAtRAC8*	This study
62	pSY30	*pJR1138-GFPRacU*	Bracha et al., 2002
63	pSY31	*pJR1138-GFPAtrac7mS*^{206}	This study
64	pSY34	*pJR1138-GFPAtrac8mS*^{205}	This study
65	pSY29	*pJR1138-GFPAtraUmS*^{266}	Bracha et al., 2002
66	pET28-a		Novagen
67	pSY113	*pET28a-RacU*	This study
68	pSY111	*pET28a-AtRAC8*	This study
69	pSY170	*pET28a-Atrac8mSS*$^{199+205}$	This study

Table 2. Primers Used in This Study

Primer Name	Sequence
SYP111	GCTCTAGACTCGAGTCAATTCTTCCCACACAGAAT
SYP112	GCTCTAGACTCGAGTCAATTCTTCCCACTCAGAATGTT
SYP124	CCGCTCGAGTCTAGATTACATCAACAAGCTGCGACGCTC
SYP125	CCGCTCGAGTCTAGATTACATCAACAAGCTGCGACGCTC
SYP127	CCGCTCGAGTCTAGATCAATGCCGAGTCACTATCCT
SYP128	GGAGCGAGCTCCATATGGCTTCGAGTGCTTCAAAATTC
SYP129	CATATGGAGCTCGCAGATGCAAACGAAGTAGTG
SYP130	CATATGGAGCTCGCTTCAAGTGCTTCAAAGTTC
SYP135	CCGCTCGAGTCTAGATCAATGCCGAGTCACTATCCTCCCACTCAGAACATT
SYP136	ACGGCAGTTTATCAAATGTTC
SYP137	TAAACTGCCGTGATTCGACTT
SYP142	CATATGGAGCTCAGTGCTTCGAAGTTCATAAAA
SYP143	CCGCTCGAGTCTAGATTAAGCAGCGGTGCAACCTCC
SYP144	CCGCTCGAGTCTAGATTAAGCAGCGGTGCTACCTCCACA
SYP145	GCGGAAGTCTCTCAAACATTCT
SYP146	AGAGACTTCCGCTGCGAGG
SYP147	GCTCTAGACTCGAGTTACTTCCCACACAGAATGTTTGA
SYP149	GGCTCTAGATCAATGCCGAGTCACATTCTTCCCACACAGAATGTT
SYP150	GCAGATCTAGATTAAGCAGCGGTGCTACCTCCACTGACAATACTC
SYP151	GCAGATCTAGATCAAGCGGTGCAACCTCCACAGAC
SYP155	TGTTACTGTTGGAGATGTGGCTGTTGGGAAGACATG
SYP156	CATGTCTTCCCAACAGCCACATCTCCAACAGTAACA
SYP160	ATAGAAGATCCGGTAGCTCCATTGCGAGTATTG
SYP161	CAATACTCGCAATGGAGCTACCGGATCTTCTATG

propriate plasmids. Cultures (10 mL) were grown overnight at 28°C in Luria-Bertani liquid medium with kanamycin (30 μg/mL). The next day, 500-μL cultures were transferred into an induction medium (50.78 mM Mes, 0.5% Glc, 1.734 mM NaH_2PO_4, 0.2 mM acetosyringone, and 5% 20X-AB mix [20X-AB mix is 373.9 mM NH_4Cl, 24.34 mM $MgSO_4$, 40.23 mM KCl, 1.36 mM $CaCl_2$, and 0.18 mM $FeSO_4 \cdot 7H_2O$]) and grown for an additional 6 h until OD_{600} reached 0.2 to 0.8. Before injection, cultures were diluted with induction medium until OD_{600} reached 0.2. Leaves were observed for GFP fluorescence at 24 to 48 h after injection.

Table 3. Primer Sets and Methods Used to Create Site-Directed Mutations

Gene	5′; 3′ Oligonucleotide Primers	Template	Mutagenesis Method[a]
AtRAC7	PSY142; PSY143	Flower cDNA library	–
AtRAC8	PSY128; PSY111	Flower cDNA library	–
AtRAC10	PSY130; PSY127	Flower cDNA library	–
RacU	PSY129; PSY124	EST (G.B U88402)	–
Atrac7mS^{206}	PSY142; PSY144	*AtRAC7*	1
Atrac8mS^{205}	PSY128; PSY112	*AtRAC8*	1
Atrac10mS^{208}	PSY130; PSY135	*AtRAC10*	1
racUmS	PSY129; PSY125	*RACU*	1
Atrac7mS^{203}	PSY142; PSY143	*Atrac7mSS*$^{203+206}$	1
Atrac7mS^{196}	PSY160; PSY161	*AtRAC7*	3
Atrac8mS^{199}	I) PSY145; PSY146	I) *AtRAC8*	2
	II) PSY128; PSY111	II) First-step product	
Atrac10mS^{202}	I) PSY136; PSY137	I) *AtRAC10*	2
	II) PSY130; PSY127	II) First-step product	
Atrac7mSS$^{203+206}$	PSY142; PSY150	*AtRAC7*	1
Atrac8mSS$^{199+205}$	PSY128; PSY112	*Atrac8mS*^{199}	1
Atrac10mSS$^{202+208}$	PSY130; PSY135	*Atrac10mS*^{202}	1
Atrac7mCaa^{-}	PSY142; PSY150	*AtRAC7*	1
Atrac8mCaa^{-}	PSY128; PSY147	*AtRAC8*	1
Atrac8m10C′	PSY128; PSY149	*AtRAC8*	1
Atrac7mV^{15}	PSY155; PSY156	*AtRAC7*	3

[a] 1, direct PCR; 2, sequential PCR steps; 3, use of the QuikChange Kit.

4′,6-Diamidino-2-Phenylindole Staining

A peace of leaf was dipped in 1 M KCl and then incubated in 100 μg/mL 4′,6-diamidino-2-phenylindole (Sigma) for 30 min at 4°C.

Plasmolysis

Leaves were plasmolyzed by incubation in 30% glycerol. Leaf sections were mounted on microscope slides in the plasmolysis solution.

Stable Transformations of Arabidopsis

To create GFPAtRAC8-expressing transgenic plants, wild-type Columbia Arabidopsis plants were transformed using the floral dip method. Analysis was performed on T2 kanamycin-resistant seedlings germinated in sterile water containing 50 μg/mL kanamycin. Five-day-old seedlings were taken for analysis.

Yeast Expression

Plasmids 2, 3, 5 to 7, and 9 were digested with XbaI and EcoRV, treated with Klenow DNA polymerase, and cloned subsequently into yeast shuttle vector pJR1138 (Yalovsky et al., 1997) to create plasmids 60 to 65. All yeast strains used in this study are listed in Table 4. Yeast transformation was performed using a standard lithium acetate transformation protocol.

Bacterial Expression

RacU was subcloned into pET28-a (Novagen, Madison, WI) to create plasmid 67. For protein expression, the plasmid was transformed into *E. coli* BL23. AtRAC8 and Atrac8mSS$^{199+205}$ were subcloned into pET28-a (Novagen) to create plasmids 68 and 69. For protein expression, the plasmids were transformed into *E. coli* BL21 CodonPlus (DE3) RIL (Stratagene). Cells were grown to an OD_{600} of 0.6, and protein expression was induced by adding 2 mM isopropylthio-β-galactoside. Purification on nickel–nitrilotriacetic acid agarose

Table 4. Yeast Strains Used in This Study

Strain	Genotype	Source or Reference
JRY 6958	*MATa his3 leu2 met15 ura3 pep4Δ*::KanMX	Rine laboratory
CTY716	*MATa ade2 lys2 his3 trp1 leu2 ura3 ram1Δ*::*ADE2*	Yalovsky et al., 1997
SYY105	*MATa ade2 lys2 his3 trp1 leu2 ura3 ram1Δ*::*ADE2* (pSYYFTA1 [high-copy-number *URA3*, *LeFTA*]), pSYFTB2 [high-copy-number *TRP1*, *LeFTB*])	Yalovsky et al., 1997
SYY300	*MATa ade2 lys2 his3 trp1 leu2 ura3 ram1Δ*::*ADE2* (pSYYFTA1 [high-copy-number *URA3AtGGTA*]), pSYFTB2 [high-copy-number *TRP1*, *AtGGTB*])	Transformant of CTY716; this study
SYY515	*MATa ade2 lys2 his3 trp1 leu2 ura3 ram1Δ*::*ADE2* (pSYYFTA1 [high-copy-number *URA3*, *LeFTA*]), pSYFTB2 [high-copy-number *TRP1*, *LeFTB*]) + pSY32	Transformant of SYY105; this study
SYY516	*MATa ade2 lys2 his3 trp1 leu2 ura3 ram1Δ*::*ADE2* (pSYYFTA1 [high-copy-number *URA3*, *LeFTA*]), pSYFTB2 [high-copy-number *TRP1*, *LeFTB*]) + pSY33	Transformant of SYY105; this study
SYY517	*MATa ade2 lys2 his3 trp1 leu2 ura3 ram1Δ*::*ADE2* (pSYYFTA1 [high-copy-number *URA3*, *LeFTA*]), pSYFTB2 [high-copy-number *TRP1*, *LeFTB*]) + pSY31	Transformant of SYY105; this study
SYY518	*MATa ade2 lys2 his3 trp1 leu2 ura3 ram1Δ*::*ADE2* (pSYYFTA1 [high-copy-number *URA3*, *LeFTA*]), pSYFTB2 [high-copy-number *TRP1*, *LeFTB*]) + pSY34	Transformant of SYY105; this study
SYY519	*MATa ade2 lys2 his3 trp1 leu2 ura3 ram1Δ*::*ADE2* + pSY32	Transformant of CTY716; this study
SYY515	*MATa ade2 lys2 his3 trp1 leu2 ura3 ram1Δ*::*ADE2* + pSY33	Transformant of CTY716; this study
SYY516	*MATa ade2 lys2 his3 trp1 leu2 ura3 ram1D*::*ADE2* + pSY31	Transformant of CTY716; this study
SYY517	*MATa ade2 lys2 his3 trp1 leu2 ura3 ram1Δ*::*ADE2* + pSY34	Transformant of CTY716; this study
SYY301	*MATa ade2 lys2 his3 trp1 leu2 ura3 ram1Δ*::*ADE2* (pSYYFTA1 [high-copy-number *URA3AtGGTA*]), pSYFTB2 [high-copy-number *TRP1*, *AtGGTB*]) + pSY32	Transformant of SYY300; this study
SYY302	*MATa ade2 lys2 his3 trp1 leu2 ura3 ram1Δ*::*ADE2* (pSYYFTA1 [high-copy-number *URA3AtGGTA*]), pSYFTB2 [high-copy-number *TRP1*, *AtGGTB*]) + pSY33	Transformant of SYY300; this study
SYY303	*MATa ade2 lys2 his3 trp1 leu2 ura3 ram1Δ*::*ADE2* (pSYYFTA1 [high-copy-number *URA3AtGGTA*]), pSYFTB2 [high-copy-number *TRP1*, *AtGGTB*]) + pSY31	Transformant of SYY300; this study
SYY304	*MATa ade2 lys2 his3 trp1 leu2 ura3 ram1Δ*::*ADE2* (pSYYFTA1 [high-copy-number *URA3AtGGTA*]), pSYFTB2 [high-copy-number *TRP1*, *AtGGTB*]) + pSY34	Transformant of SYY300; this study
SYY508	*MATa his3 leu2 met15 ura3 pep4Δ*::KanMX + pSY30	Transformant of JRY 6958
SYY511	*MATa his3 leu2 met15 ura3 pep4Δ*::KanMX + pSY29	Transformant of JRY 6958

columns was performed according to the manufacturer's instructions (Qiagen, Valencia, CA).

In Vitro Prenylation Assays

Prenylation assays were performed as described previously (Caldelari et al., 2001).

In Vitro Palmitoylation Assays

In vitro palmitoylation reactions were performed essentially as described previously (Veit, 2000; Webb et al., 2000). ^{3}H-Palmitate was converted to ^{3}H-palmitoyl-CoA by incubation of the former in the presence of CoA and acyl-CoA synthetase (Fluka, Milwaukee, WI). Palmitoylation was performed by incubating recombinant AtRAC8 and Atrac8mSS$^{199+205}$ with ^{3}H-palmitoyl-CoA in the presence or absence of 1 mM 2-bromopalmitate. After incubation for 1 h at 28°C, proteins were precipitated from unbound material with a 1:1 solution of chloroform:methanol (v/v) and subjected to centrifugation for 10 min at 10,000*g*. Pellets were washed with methanol before denaturation in SDS-PAGE sample buffer (Laemmli, 1970) that did not contain a reducing agent (Linder et al., 1995). After denaturation, proteins were resolved by SDS-PAGE and then fixed, fluorographed with Amplify reagent (Amersham), and exposed to x-ray film (Kodak XAR). Typically, films were exposed for 3 to 5 days.

Inhibition of Palmitoylation

To determine whether AtRAC7, AtRAC8, and AtRAC10 are palmitoylated, cultures were injected into the leaves together with either 1 mM of the protein palmitoylation inhibitor 2-bromopalmitate (Fluka) dissolved in 10% DMSO or 10% DMSO alone. Leaf injections were performed as described above.

Protein Immunoblot Analysis

Proteins from leaves that expressed GFPAtRAC8, GFPAtrac8mSS$^{199+205}$, GFPAtRAC7, GFPAtrac7mSS$^{203+206}$, GFPAtRAC10, or free GFP were extracted in 10 mM Hepes-KOH, pH 7.5, 10 mM EDTA, 1 mM DTT, and plant protease inhibitor mix (Sigma). To precipitate insoluble material, extracts were centrifuged at 18,000*g*. The resulting supernatant was collected and centrifuged again at 100,000*g* for 2 h. The insoluble pellet was incubated on ice for 20 min in 50 mM Hepes-KOH, pH 7.5, 50 mM NaCl, 1% deoxycholic acid, 1% Triton X-100, 0.5% SDS, 1 mM DTT, and protease inhibitor mix. The extract was centrifuged again at 18,000*g* for 10 min. Supernatant was collected for further analyses. Proteins were resolved by SDS-PAGE (Laemmli, 1970) and transferred onto nitrocellulose membranes. Membranes were incubated for 1 h at room temperature with mouse anti-GFP monoclonal antibodies (Stressgen, San Diego, CA) and then washed and incubated with blotting-grade horseradish peroxidase–conjugated goat anti-mouse secondary antibodies (Bio-Rad). Detection was performed using SuperSignal (Pierce). Before gel electrophoresis, deoxycholate, Triton X-100, and SDS were added to the 100,000*g* supernatant, resulting in the final concentrations used to solubilize the membranes.

Fluorescence and Confocal Imaging

Wide-field fluorescence imaging was performed using a Zeiss Axioplan-2 imaging fluorescence microscope (Jena, Germany) equipped with an AxioCam cooled charge-coupled device camera. Confocal imaging was performed using a Zeiss R510 confocal laser scanning microscope. Excitation was performed with an argon laser set to 488 nm, and emission was detected with a 525-nm ± 15-nm band-path filter. Image analysis was performed with Zeiss AxioVision, Zeiss CLSM-5, and Adobe Photoshop 6.0 (Mountain View, CA).

Upon request, all novel materials described in this article will be made available in a timely manner for noncommercial research purposes. No restrictions or conditions will be placed on the use of any materials described in this article that would limit their use for noncommercial research purposes.

Accession Numbers

The GenBank accession numbers for the genes mentioned in this article are as follows: *AtRAC7* (AF079484), *AtRAC8* (AF079486), *AtRAC10* (AF079485), and *RacU* (U88402).

ACKNOWLEDGMENTS

We thank A. Barbul and Z. Offir for technical assistance, G. Sagi and O. Gelbart-Liarzi for materials, and R. Freedman for editing. This research was supported by grants from the Binational Agricultural Research and Development Fund (IS-3215-01), the Binational Science Foundation (1999423), and the Israel Science Foundation (571/99-3) to S.Y.

Received June 21, 2002; accepted July 4, 2002.

REFERENCES

Apolloni, A., Prior, I.A., Lindsay, M., Parton, R.G., and Hancock, J.F. (2000). H-ras but not K-ras traffics to the plasma membrane through the exocytic pathway. Mol. Cell. Biol. **20,** 2475–2487.

Ausubel, F.M., Brent, R., Kingston, R.E., Moore, D.D., Seidman, J.G., Smith, J.A., Struhl, K. (1995) Current Protocols in Molecular Biology. (New York: John Wiley and Sons Inc.).

Bar-Sagi, D., and Hall, A. (2000). Ras and Rho GTPases: A family reunion. Cell **103,** 227–238.

Bishop, A.L., and Hall, A. (2000). Rho GTPases and their effector proteins. Biochem. J. **348**, 241–255.

Bokoch, G.M. (1994). Regulation of the human neutrophil NADPH oxidase by the Rac GTP-binding proteins. Curr. Opin. Cell Biol. **6,** 212–218.

Boyartchuk, V.L., Ashby, M.N., and Rine, J. (1997). Modulation of ras and α-factor function by carboxyl-terminal proteolysis. Science **275,** 1796–1800.

Bracha, K., Lavy, M., and Yalovsky, S. (2002). The Arabidopsis AtSTE24 is a CaaX protease with broad substrate specificity. J. Biol. Chem. **277,** 29856–29864.

Buss, J.E., Solski, P.A., Schaeffer, J.P., MacDonald, M.J., and

Der, C.J. (1989). Activation of cellular p21^{ras} by myristoylation. Biochem. Soc. Trans. **17,** 867–869.

Caldelari, D., Sternberg, H., Rodriguez-Concepcion, M., Gruissem, W., and Yalovsky, S. (2001). Efficient prenylation by a plant geranylgeranyltransferase-I requires a functional CaaL box motif and a proximal polybasic domain. Plant Physiol. **126,** 1416–1429.

Choy, E., Chiu, V.K., Silletti, J., Feoktistov, M., Morimoto, T., Michaelson, D., Ivanov, I.E., and Philips, M.R. (1999). Endomembrane trafficking of Ras: The CaaX motif targets proteins to the ER and Golgi. Cell **98,** 69–80.

Cutler, S., Ghassemian, M., Bonetta, D., Cooney, S., and McCourt, P. (1996). A protein farnesyl transferase involved in abscisic acid signal transduction in Arabidopsis. Science **273,** 1239–1241.

Feron, O., Saldana, F., Michel, J.B., and Michel, T. (1998). The endothelial nitric-oxide synthase-caveolin regulatory cycle. J. Biol. Chem. **273,** 3125–3128.

Fu, Y., Li, H., and Yang, Z. (2002). The ROP2 GTPase controls the formation of cortical fine F-actin and the early phase of directional cell expansion during Arabidopsis organogenesis. Plant Cell **14,** 777–794.

Fu, Y., Wu, G., and Yang, Z. (2001). Rop GTPase-dependent dynamics of tip-localized F-actin controls tip growth in pollen tubes. J. Cell Biol. **152,** 1019–1032.

Hall, A. (1998). Rho GTPases and the actin cytoskeleton. Science **279,** 509–514.

Ivanchenko, M., Vejlupkova, Z., Quatrano, R.S., and Fowler, J.E. (2000). Maize ROP7 GTPase contains a unique, CaaX box-independent plasma membrane targeting signal. Plant J. **24,** 79–90.

James, G.L., Goldstein, J.E., and Brown, S.K. (1995). Polylysine and CVIM sequences of K-RasB dictate specificity of prenylation and confer resistance to benzodiazepine peptidomimetic *in vitro*. J. Biol. Chem. **270,** 6221–6226.

Jones, M.A., Shen, J.-J., Fu, Y., Li, H., Yang, Z., and Grierson, C.S. (2002). The Arabidopsis Rop2 GTPase is a positive regulator of both root hair initiation and tip growth. Plant Cell **14,** 763–776.

Kost, B., Lemichez, E., Spielhofer, P., Hong, Y., Tolias, K., Carpenter, C., and Chua, N.H. (1999). Rac homologues and compartmentalized phosphatidylinositol 4,5-bisphosphate act in a common pathway to regulate polar pollen tube growth. J. Cell Biol. **145,** 317–330.

Laemmli, U.K. (1970). Cleavage of structural proteins during the assembly of the head of bacteriophage T4. Nature **227,** 680–685.

Larkin, J.C., Marks, M.D., Nadeau, J., and Sack, F. (1997). Epidermal cell fate and patterning in leaves. Plant Cell **9,** 1109–1120.

Li, H., Lin, Y., Heath, R.M., Zhu, M.X., and Yang, Z. (1999). Control of pollen tube tip growth by a Rop GTPase-dependent pathway that leads to tip-localized calcium influx. Plant Cell **11,** 1731–1742.

Li, H., Shen, J.J., Zheng, Z.L., Lin, Y., and Yang, Z. (2001). The rop GTPase switch controls multiple developmental processes in Arabidopsis. Plant Physiol. **126,** 670–684.

Lin, Y., Wang, Y., Zhu, J.-K., and Yang, Z. (1996). Localization of a Rho GTPase implies a role in tip growth and movement of the generative cell in pollen tubes. Plant Cell **8,** 293–303.

Linder, M.E. (2000). Reversible modification of proteins with thioester-linked fatty acids. In Protein Lipidation, F. Tamanoi and D.S. Sigman, eds (San Diego, CA: Academic Press), pp. 215–240.

Linder, M.E., Kleuss, C., and Mumby, S.M. (1995). Palmitoylation of G-protein α subunit. Methods Enzymol. **250,** 314–330.

Michaelson, D., Silletti, J., Murphy, G., D'Eustachio, P., Rush, M., and Philips, M.R. (2001). Differential localization of Rho GTPases in live cells: Regulation by hypervariable regions and RhoGDI binding. J. Cell Biol. **152,** 111–126.

Molendijk, A.J., Bischoff, F., Rajendrakumar, C.S., Friml, J., Braun, M., Gilroy, S., and Palme, K. (2001). *Arabidopsis thaliana* Rop GTPases are localized to tips of root hairs and control polar growth. EMBO J. **20,** 2779–2788.

Mumby, S.M. (1997). Reversible palmitoylation of signaling proteins. Curr. Opin. Cell Biol. **9,** 148–154.

Mumby, S.M., Kleuss, C., and Gilman, A.G. (1994). Receptor regulation of G-protein palmitoylation. Proc. Natl. Acad. Sci. USA **91,** 2800–2804.

Olofsson, B. (1999). Rho guanine dissociation inhibitors: Pivotal molecules in cellular signalling. Cell. Signal. **11,** 545–554.

Ono, E., Wong, H.L., Kawasaki, T., Hasegawa, M., Kodama, O., and Shimamoto, K. (2001). Essential role of the small GTPase Rac in disease resistance of rice. Proc. Natl. Acad. Sci. USA **98,** 759–764.

Park, J., Choi, H.J., Lee, S., Lee, T., Yang, Z., and Lee, Y. (2000). Rac-related GTP-binding protein in elicitor-induced reactive oxygen generation by suspension-cultured soybean cells. Plant Physiol. **124,** 725–732.

Peskan, T., Westermann, M., and Oelmuller, R. (2000). Identification of low-density Triton X-100 insoluble plasma membrane microdomains in higher plants. Eur. J. Biochem. **267,** 6989–6995.

Potikha, T.S., Collins, C.C., Johnson, D.I., Delmer, D.P., and Levine, A. (1999). The involvement of hydrogen peroxide in the differentiation of secondary walls in cotton fibers. Plant Physiol. **119,** 849–858.

Resh, M.D. (1999). Fatty acylation of proteins: New insights into membrane targeting of myristoylated and palmitoylated proteins. Biochim. Biophys. Acta **1451,** 1–16.

Rodriguez-Concepcion, M., Toledo-Ortiz, G., Yalovsky, S., Caldelari, D., and Gruissem, W. (2000). Carboxyl-methylation of prenylated calmodulin CaM53 is required for efficient plasma membrane targeting of the protein. Plant J. **24,** 775–784.

Rodriguez-Concepcion, M., Yalovsky, S., and Gruissem, W. (1999a). Protein prenylation in plants: Old friends and new targets. Plant Mol. Biol. **39,** 865–870.

Rodriguez-Concepcion, M., Yalovsky, S., Zik, M., Fromm, H., and Gruissem, W. (1999b). The prenylation status of a novel plant calmodulin directs plasma membrane or nuclear localization of the protein. EMBO J. **18,** 1996–2007.

Sachs, T. (1991). Pattern formation in plant tissues. In Developmental and Cell Biology Series. P.W. Barlow, D. Bran, P.B. Green, and J.M.W. Slack, eds (Cambridge: Cambridge University Press).

Schafer, W.R., and Rine, J. (1992). Protein prenylation: Genes, enzymes, targets and functions. Annu. Rev. Genet. **30,** 209–237.

Schiene, K., Puhler, A., and Niehaus, K. (2000). Transgenic tobacco plants that express an antisense construct derived from a *Medicago sativa* cDNA encoding a Rac-related small GTP-binding protein fail to develop necrotic lesions upon elicitor infiltration. Mol. Gen. Genet. **263,** 761–770.

Takahashi, K., Sasaki, T., Mammoto, A., Takaishi, K., Kameyama, T., Tsukita, S., and Takai, Y. (1997). Direct interaction of the Rho GDP dissociation inhibitor with ezrin/radixin/moesin initiates the activation of the Rho small G protein. J. Biol. Chem. **272,** 23371–23375.

Trainin, T., Shmuel, M., and Delmer, D.P. (1996). In vitro prenylation of the small GTPase Rac13 in cotton. Plant Physiol. **112,** 1491–1497.

Trotochaud, A.E., Hao, T., Wu, G., Yang, Z., and Clark, S.E. (1999). The CLAVATA1 receptor-like kinase requires CLAVATA3

for its assembly into a signaling complex that includes KAPP and a Rho-related protein. Plant Cell **11,** 393–406.

Van Aelst, L., and D'Souza-Schorey, C. (1997). Rho GTPases and signaling networks. Genes Dev. **11,** 2295–2322.

Veit, M. (2000). Palmitoylation of the 25-kDa synaptosomal protein (SNAP-25) in vitro occurs in the absence of an enzyme, but is stimulated by binding to syntaxin. Biochem. J. **345,** 145–151.

Veit, M., Laage, R., Dietrich, L., Wang, L., and Ungermann, C. (2001). Vac8p release from the SNARE complex and its palmitoylation are coupled and essential for vacuole fusion. EMBO J. **20,** 3145–3155.

Webb, Y., Hermida-Matsumoto, L., and Resh, M.D. (2000). Inhibition of protein palmitoylation, raft localization, and T cell signaling by 2-bromopalmitate and polyunsaturated fatty acids. J. Biol. Chem. **275,** 261–270.

Wedegaertner, P.B., and Bourne, H.R. (1994). Activation and depalmitoylation of Gs alpha. Cell **77,** 1063–1070.

Willumsen, B.M., Cox, A.D., Solski, P.A., Der, C.J., and Buss, J.E. (1996). Novel determinants of H-Ras plasma membrane localization and transformation. Oncogene **13,** 1901–1909.

Winge, P., Brembu, T., Kristensen, R., and Bones, A.M. (2000). Genetic structure and evolution of RAC-GTPases in *Arabidopsis thaliana*. Genetics **156,** 1959–1971.

Wolven, A., Okamura, H., Rosenblatt, Y., and Resh, M.D. (1997). Palmitoylation of $p59^{fyn}$ is reversible and sufficient for plasma membrane association. Mol. Biol. Cell **8,** 1159–1173.

Xu, X., Bittman, R., Duportail, G., Heissler, D., Vilcheze, C., and London, E. (2001). Effect of the structure of natural sterols and sphingolipids on the formation of ordered sphingolipid/sterol domains (rafts). J. Biol. Chem. **276,** 33540–33546.

Yalovsky, S., Rodriguez-Concepcion, M., and Gruissem, W. (1999). Lipid modifications of proteins: Slipping in and out of membranes. Trends Plant Sci. **4,** 439–445.

Yalovsky, S., Trueblood, C.E., Callan, K.L., Narita, J.O., Jenkins, S.M., Rine, J., and Gruissem, W. (1997). Plant farnesyltransferase can restore yeast Ras signaling and mating. Mol. Cell. Biol. **17,** 1986–1994.

Yeh, D.C., Duncan, J.A., Yamashita, S., and Michel, T. (1999). Depalmitoylation of endothelial nitric-oxide synthase by acyl-protein thioesterase 1 is potentiated by Ca^{2+}-calmodulin. J. Biol. Chem. **274,** 33148–33154.

Zacharias, D.A., Violin, J.D., Newton, A.C., and Tsien, R.Y. (2002). Partitioning of lipid-modified monomeric GFPs into membrane microdomains of live cells. Science **296,** 913–916.

Zhang, F.L., and Casey, P.J. (1996). Protein prenylation: Molecular mechanisms and functional consequences. Annu. Rev. Biochem. **65,** 241–269.

Zheng, Z.L., and Yang, Z. (2000a). The Rop GTPase: An emerging signaling switch in plants. Plant Mol. Biol. **44,** 1–9.

Zheng, Z.L., and Yang, Z. (2000b). The Rop GTPase switch turns on polar growth in pollen. Trends Plant Sci. **5,** 298–303.